

Inferring information from the S&P 500 and CBOE indices:

The more the merrier?*

Jiling Cao

School of Engineering, Computer and Mathematical Sciences

Auckland University of Technology

Private Bag 92006, Auckland 1142, New Zealand

Email: jiling.cao@aut.ac.nz

Xinfeng Ruan

Department of Accountancy and Finance

Otago Business School, University of Otago

Dunedin 9054, New Zealand

Email: xinfeng.ruan@otago.ac.nz

Wenjun Zhang

School of Engineering, Computer and Mathematical Sciences

Auckland University of Technology

Private Bag 92006, Auckland 1142, New Zealand

Email: wenjun.zhang@aut.ac.nz

First Draft: 12 October 2018

This Draft: 06 March 2019

*Please send correspondence to Xinfeng Ruan, Department of Accountancy and Finance, Otago Business School, University of Otago, Dunedin 9054, New Zealand; telephone +64 3 479 8315. Email: xinfeng.ruan@otago.ac.nz. We declare that we have no relevant or material financial interests that relate to the research described in this paper. All remaining errors are ours.

Inferring information from the S&P 500 and CBOE indices: The more the merrier?

Abstract

The Chicago Board Options Exchange (CBOE) updated the CBOE Volatility Index (VIX) in 2003 and further launched the CBOE Skew Index (SKEW) in 2011, in order to measure the 30-day risk-neutral volatility and skewness of the S&P 500 Index (SPX). This paper mainly compares the information extracted from the SPX and CBOE indices in terms of the SPX option pricing performance. Based on our empirical analysis, VIX is a very informative index for option prices. Whether adding the SKEW or the VIX term structure can improve the option pricing performance depends on the model we choose. Roughly speaking, the VIX term structure is informative for some models, while, the SKEW is very noisy and does not contain much important information for option prices.

Keywords: SPX; VIX; SKEW; option pricing; term structure; MCMC; affine model.

JEL Classifications: G12; G13.

1. Introduction

The Chicago Board Options Exchange (CBOE) introduced the old CBOE Volatility Index (VXO) in 1993 to measure the market's expectation of 30-day volatility implied by S&P 100 Index option prices. In 2003, the CBOE launched the new CBOE Volatility Index (VIX) by supplying a script for replicating volatility exposure with a portfolio of the S&P 500 Index (SPX) options. The new method estimates expected volatility by averaging the weighted prices of SPX puts and calls over a wide range of strike prices. It is colloquially referred to as the fear index or the fear gauge. In addition to the VIX, CBOE also published the 9-Day Volatility Index (VIX9D), the 3-Month Volatility Index (VIX3M) and the 6-Month Volatility Index (VIX6M) on the SPX Index.

Documented by Jiang and Tian (2005), the model-free volatility subsumes all information contained in the Black-Scholes implied volatility and past realized volatility and is a more efficient forecast for the future realized volatility. Lin (2007) implements a generalized method of moments (GMM) to estimate the model parameters in both physical and riskneutral probability measures by using the VIX and 5-minute-based integrated volatilities and documents that the VIX is very informative for VIX futures prices. In order to avoid the computational burden associated with option valuation, Duan and Yeh (2010) obtain the model parameters and the latent stochastic volatility from the maximum likelihood estimates (MLEs) under a jump-diffusion model. This takes the advantage that the VIX is a linear function of the latent stochastic volatility, so that it is possible to obtain the joint likelihood function of the SPX return and the VIX. Furthermore, Zhu and Lian (2012); Kaeck and Alexander (2012) and Yang and Kannianen (2017) use the Markov chain Monte Carlo (MCMC) method to simultaneously estimate the model parameters in both physical and risk-neutral probability measures and the latent variables by using the SPX and VIX data. Zhu and Lian (2012) and Yang and Kannianen (2017) infer information from the SPX and 30-day VIX indices under an affine jump-diffusion model and non-affine Lévy model, respectively, while Kaeck and Alexander (2012) extract the information from the SPX, 30-day VIX and 360-day VIX indices. All of the above studies investigate pricing performance under the different continuous-time models calibrated by using the same data set. In contrast to them, we explore option pricing

performance for the models calibrated by using the different data sets. Our studies raise an important question of whether adding new index can really improve the option pricing performance.

In order to capture the curve of implied volatilities with a shape of “smirk” or “skew”, implied by the SPX option prices, the CBOE launched the CBOE Skew Index (SKEW) in February 2011. The index value typically reflects trading activity of portfolio managers hedging tail risk with options, to protect portfolios from a large, sudden decline in the market (i.e., a black swan event or market crash). Similar to the VIX, the SKEW measures the perceived tail risk of the distribution of SPX returns over a 30-day horizon by using the model-free method in Bakshi, Kapadia, and Madan (2003). Zhang, Zhen, Sun, and Zhao (2017) provide an exact formula for the skewness of stock returns implied in the Heston (1993) model and separately use the SPX return, the CBOE VIX and SKEW term structures to calibrate the model. Unfortunately, they do not study the option pricing performance after adding the SKEW information. Recently, Liu and van der Heijden (2016) find that the estimation errors of true skewness by using the CBOE SKEW method are very large. In this paper, we further investigate whether adding the SKEW can improve models’ option pricing performance.

In this paper, we consider three typical models. The first model is the stochastic volatility model with contemporaneous jumps in returns and volatility (SVCJ), which is the most popular affine model in the literature, e.g., Bakshi, Cao, and Chen (1997); Eraker, Johannes, and Polson (2003); Eraker (2004); Broadie, Chernov, and Johannes (2007); Lin and Chang (2010); Duan and Yeh (2010); Neuberger (2012); Zhu and Lian (2011, 2012); Neumann, Prokopczuk, and Simen (2016); Kaeck, Rodrigues, and Seeger (2017); Ruan and Zhang (2018); Da Fonseca and Ignatieva (2019) and others. Bakshi et al. (1997); Eraker (2004); Broadie et al. (2007) and Neumann et al. (2016) document that the SVCJ model is good enough to fit options and returns data simultaneously. According to the empirical observation in Bates (2006), i.e., more jumps occur during more volatile periods, we adopt the second model from Bates (2006) and Aït-Sahalia, Karaman, and Mancini (2015). The second model, the SVCJ model with stochastic jump intensity, is labeled as “SCVJI”. The jump intensity is a linear function of the spot variance. The SCVJI model is very popular in asset pricing, e.g., Eraker and Shaliastovich (2008); Drechsler and Yaron (2010); Drechsler (2013) and Jin

(2014). Recently, Du and Luo (2017) find that jump propagation (i.e., the phenomenon in which the strike of one jump substantially raises the probability for more to follow) dominates the jump risks from the joint time series of SPX and its options and use a two-factor Hawkes jump-diffusion model to capture jump propagation. Therefore, the last model we consider is the SVCJ model with Hawkes process (SVCJH). Du and Luo (2017) further document that the SVCJH can explain well the pronounced smirk pattern in option implied volatility, which is modelled as the SKEW in this paper.

As Kaeck and Alexander (2012) have documented that the SVCJ model with the stochastic long-term level in the volatility (i.e., two-factor SVCJ model, labeled as J2-A2 in Kaeck and Alexander (2012)) has larger out-of-sample option pricing errors than the SVCJ model (labeled as J2-A1 in Kaeck and Alexander (2012)), in this paper, we do not consider the two-factor SVCJ model. In Kaeck and Alexander (2012) and Yang and Kannianen (2017), even the models are non-affine, the close-form solution of the VIX can be obtained. However, it is difficult to get an explicit SKEW formula under the non-affine models, as the SKEW formula relies on the moment generating function (MGF) of the log SPX return, which can be explicitly derived under affine models. In order to get the close-form solution for the SKEW, we focus on the affine models in Duffie, Pan, and Singleton (2000) rather than the non-affine models.

In line with Zhu and Lian (2012); Kaeck and Alexander (2012) and Yang and Kannianen (2017), we use MCMC method to calibrate the models as the MCMC method has sampling properties superior to other methods documented in the literature. Comparing with the MLEs in Duan and Yeh (2010), the MCMC method can handle more complex data, which are no longer a linear function of latent variables, like option data in Eraker (2004) and SKEW data in this paper. It allows us directly get the latent variables through the MCMC procedure. Furthermore, Jacquier, Polson, and Rossi (2002) show that the MCMC method works better than the MLEs in terms of estimating parameter of stochastic volatility models.

The main contribution in this paper is to newly investigate whether adding the VIX term structure and SKEW data to a model can improve model's option pricing performance. The answer depends on the model we choose. Roughly speaking, the VIX is a very important index for option prices, while SKEW is very noisy for option prices. Adding the VIX term

structure information to a model can improve the option pricing performance only for some models.

The remainder of our article is organized as follows. Section 2 presents the framework. Section 3 introduces the data. The details of the model calibration are shown in Section 4 and the empirical results are given in Section 5. Section 6 concludes. Appendix A collects all proofs. Appendix B provides technical notes on MCMC with the CBOE SKEW and Appendix C gives the fit of CBOE indices.

2. Framework

2.1 Affine models

In this paper, we collect three different affine models introduced in Duffie et al. (2000) in order to eliminate the model bias. Under the physical probability measure \mathbb{P} , at time t , the S&P 500 Index (SPX), S_t , follows,

$$\begin{cases} \frac{dS_t}{S_t} = (r - q + \phi_t) dt + \sqrt{v_t} dW_{t,S} + (e^x - 1) dN_t - \lambda_t m dt, \\ dv_t = \kappa(\theta - v_t) dt + \sigma_v \sqrt{v_t} dW_{t,v} + y dN_t, \end{cases} \quad (1)$$

where r is risk free rate; q is the dividend yield and ϕ_t is the equity premium; $W_{t,S}$ and $W_{t,v}$ are correlated Brownian motions with correlation ρ on a probability space $(\Omega, \mathcal{F}, \mathbb{P})$; N_t is a Poisson process with jump intensity λ_t . The jump sizes $x|y \sim N(\mu_x + \rho_{Jy}, \sigma_x^2)$ and $y \sim Exp(1/\mu_y)$ with mean μ_y . In addition, $m = E[(e^x - 1)] = \frac{e^{\mu_x + \sigma_x^2/2}}{1 - \rho_{J\mu_y}} - 1$. Following Broadie et al. (2007), we assume $\phi_t = \eta^S v_t + \lambda_t m - \lambda_t^{\mathbb{Q}} m^{\mathbb{Q}}$, where $\eta^S v_t$ is the Brownian contribution to the equity premium; $\lambda_t m - \lambda_t^{\mathbb{Q}} m^{\mathbb{Q}}$ is the jump contribution; \mathbb{Q} is the risk-neutral measure and $m^{\mathbb{Q}} = E^{\mathbb{Q}}[(e^x - 1)]$.

For the jump intensity, we consider three cases as follows. (i) We first consider the stochastic volatility model with contemporaneous jumps in returns and volatility (SVCJ) in Eraker et al. (2003) and Broadie et al. (2007), i.e., $\lambda_t \equiv \lambda_1$ which is a constant. This is the most popular affine model in the literature, e.g., Bakshi et al. (1997); Lin and Chang (2010); Duan and Yeh (2010); Zhu and Lian (2011, 2012); Neuberger (2012); Neumann et al. (2016) and others. (ii) Bates (2006); Aït-Sahalia et al. (2015) find that more jumps occur during

more volatile periods and then they suggest that $\lambda_t \equiv \lambda_1 + \lambda_2 v_t$, where λ_1 and λ_2 are two positive constants. We call the SVCJ model with stochastic jump intensity as SVCJI model. (iii) Du and Luo (2017) document that the strikes of jumps substantially raise the probability for more to follow (called “jump propagation”) dominates the jump risks from the joint time series of SPX and its options and they propose a Hawkes process in the univariate case to capture jump propagation. Alternatively, we assume the jump intensity satisfies the dynamic

$$d\lambda_t = \beta(\lambda_\infty - \lambda_t)dt + z dN_t, \quad (2)$$

where $\beta > 0$ is the constant rate of exponential decay; λ_∞ is the constant reversion level; z is the size of the self-excited jump, which can be viewed as independent random variable and $z \sim Exp(1/\mu_z)$ with mean μ_z . Equation (2) shows the jump propagation, i.e., λ_t ramps up in response to the occurrences of jumps causing further jumps more likely to follow. We call the SVCJ model with a Hawkes process as SVCJH model. A summary of model specifications is given in Table 1.

Table 1: Summary of model specifications

Model	Jump intensity (λ_t)	Key references
SVCJ	λ_1	Eraker et al. (2003); Broadie et al. (2007) Eraker (2004); Bates
SVCJI	$\lambda_1 + \lambda_2 v_t$	(2006); Ait-Sahalia et al. (2015); Bardgett et al. (2018)
SVCJH	Given in Equation (2)	Du and Luo (2017)

Under the risk-neutral probability measure \mathbb{Q} , the stock process becomes

$$\begin{cases} \frac{dS_t}{S_t} = (r - q) dt + \sqrt{v_t} dW_{t,S}^{\mathbb{Q}} + (e^x - 1) dN_t - \lambda_t^{\mathbb{Q}} m^{\mathbb{Q}} dt, \\ dv_t = \kappa^{\mathbb{Q}} (\kappa\theta/\kappa^{\mathbb{Q}} - v_t) dt + \sigma_v \sqrt{v_t} dW_{t,v}^{\mathbb{Q}} + y dN_t, \end{cases} \quad (3)$$

where $W_{t,S}^{\mathbb{Q}}$ and $W_{t,v}^{\mathbb{Q}}$ are correlated Brownian motions with correlation ρ on a probability

space $(\Omega, \mathcal{F}, \mathbb{Q})$; N_t is a Poisson process with jump intensity $\lambda_t^{\mathbb{Q}}$; the jump sizes $x|y \sim N(\mu_x^{\mathbb{Q}} + \rho_J y, \sigma_x^2)$, $y \sim \text{Exp}(1/\mu_y^{\mathbb{Q}})$ with mean $\mu_y^{\mathbb{Q}}$. In addition, $m^{\mathbb{Q}} = E^{\mathbb{Q}}[e^x - 1] = \frac{e^{\mu_x^{\mathbb{Q}} + \sigma_x^2/2}}{1 - \rho_J \mu_y^{\mathbb{Q}}} - 1$. Eraker et al. (2003) and Eraker (2004) report statistically insignificant correlations between the two jump sizes and find that μ_y and the correlation between the two jump sizes play a very similar role. Broadie et al. (2007) further show that it is difficult to estimate the parameter ρ_J precisely. In the line with the literature, throughout this paper, we set $\rho_J = 0$.

Following Broadie et al. (2007), we can further denote the diffusive volatility risk premium $\eta^v = \kappa^{\mathbb{Q}} - \kappa$, the price jump risk premium $\eta^x = \mu_x - \mu_x^{\mathbb{Q}}$, the volatility jump risk premium $\eta^y = \mu_y^{\mathbb{Q}} - \mu_y$ and the jump intensity risk premium as $\eta^\lambda = \lambda_t^{\mathbb{Q}}/\lambda_t$. The jump intensity specifications for three affine models under the risk-neutral probability measure \mathbb{Q} therefore are given in Table 2.

Table 2: Jump intensity in the risk-neutral measure

Model	Jump intensity ($\lambda_t^{\mathbb{Q}}$)
SVCJ	$\lambda_1^{\mathbb{Q}} = \eta^\lambda \lambda_1$.
SVCJI	$\lambda_1^{\mathbb{Q}} + \lambda_2^{\mathbb{Q}} v_t$, where $\lambda_1^{\mathbb{Q}} = \eta^\lambda \lambda_1$ and $\lambda_2^{\mathbb{Q}} = \eta^\lambda \lambda_2$.
SVCJH	$d\lambda_t^{\mathbb{Q}} = \beta(\lambda_\infty^{\mathbb{Q}} - \lambda_t^{\mathbb{Q}})dt + z dN_t$, where $\lambda_\infty^{\mathbb{Q}} = \eta^\lambda \lambda_\infty$ and $z \sim \text{Exp}(1/\mu_z^{\mathbb{Q}})$ with mean $\mu_z^{\mathbb{Q}} = \eta^\lambda \mu_z$.

2.2 CBOE indices

According to the CBOE VIX white paper and Duan and Yeh (2010),¹ the CBOE VIX can be expressed as

$$\begin{aligned} VIX_{t,\tau}^2 &= \frac{2}{\tau} E_t^{\mathbb{Q}} \left[\int_t^{t+\tau} \left(\frac{dS_u}{S_u} - d \log S_u \right) \right] \\ &= \frac{1}{\tau} E_t^{\mathbb{Q}} \left(\int_t^{t+\tau} v_s ds \right) + \frac{2}{\tau} \left(e^{\mu_x^{\mathbb{Q}} + \sigma_x^2/2} - 1 - \mu_x^{\mathbb{Q}} \right) E_t^{\mathbb{Q}} \left(\int_t^{t+\tau} \lambda_s^{\mathbb{Q}} ds \right), \end{aligned}$$

¹See <https://www.cboe.com/micro/vix/vixwhite.pdf>

where $\tau = 30/365$ for the 30-day VIX (VIX30) and $\tau = 1$ for the 365-day VIX (VIX365).² Expressions of the VIX for three different models are given in Appendix A.1.

The CBOE SKEW is derived from the price of S&P 500 skewness. According to CBOE SKEW white paper and Bakshi et al. (2003),³ the risk-neutral skewness can be defined as

$$SKEW_{t,\tau} = \frac{E_t^{\mathbb{Q}} \left[\left(R_{t,t+\tau} - E_t^{\mathbb{Q}}[R_{t,t+\tau}] \right)^3 \right]}{\left(E_t^{\mathbb{Q}} \left[\left(R_{t,t+\tau} - E_t^{\mathbb{Q}}[R_{t,t+\tau}] \right)^2 \right] \right)^{3/2}} = \frac{k_3}{k_2^{3/2}}, \quad (4)$$

where the time to maturity $\tau = 30/365$; $R_{t,t+\tau} = \log \frac{S_{t+\tau}}{S_t} = X_{t+\tau} - X_t$ is the 30-day log-return of the SPX and $X_t = \log S_t$; k_2 and k_3 are the risk-neutral second and third cumulants of $R_{t,t+\tau}$, respectively.

The moment generating function (MGF) of the log SPX at time t , $f(\omega, \tau) = E_t^{\mathbb{Q}}[e^{\omega X_{t+\tau}}]$, is given in Appendix A.2. Similarly, the MGF of the log SPX return, $M(\omega, \tau) = E_t^{\mathbb{Q}}[e^{\omega R_{t,t+\tau}}]$, is obtained by

$$M(\omega, \tau) = E_t^{\mathbb{Q}}[e^{\omega R_{t,t+\tau}}] = e^{-\omega X_t} E_t^{\mathbb{Q}}[e^{\omega X_{t+\tau}}] = e^{-\omega X_t} f(\omega, \tau). \quad (5)$$

The cumulant generating function (CGF) of $R_{t+\tau}$ is the log of the MGF, i.e.,

$$K(\omega, \tau) = \log E_t^{\mathbb{Q}}[e^{\omega R_{t,t+\tau}}] = \log M(\omega, \tau) = \log f(\omega, \tau) - \omega X_t. \quad (6)$$

Based on that, the cumulants can be calculated by using the CGF,

$$k_n = \left. \frac{\partial^n K(\omega, \tau)}{\partial \omega^n} \right|_{\omega=0}, n = 2, 3. \quad (7)$$

For example, under the SVCJH model, the CGF of $R_{t+\tau}$ in (6) becomes

$$K(\omega, \tau) = A(\omega, \tau) + B(\omega, \tau)v_t + C(\omega, \tau)\lambda_t^{\mathbb{Q}}, \quad (8)$$

²Note that the terms, VIX and VIX30, are often used synonymously throughout this paper.

³See <https://www.cboe.com/micro/skew/documents/skewwhitepaperjan2011.pdf>

and the second and third cumulants of $R_{t,t+\tau}$ in (7) can be represented by

$$k_2 = A_2 + B_2 v_t + C_2 \lambda_t^{\mathbb{Q}}, \quad k_3 = A_3 + B_3 v_t + C_3 \lambda_t^{\mathbb{Q}}, \quad (9)$$

where $Z_i = \frac{\partial^i Z(\tau, \omega)}{\partial \omega^i} \Big|_{\omega=0}$ for $= \{A, B, C\}$ and $i = \{2, 3\}$.

Finally, the CBOE SKEW (4) under the SVCJH model can be solved as

$$SKEW_{t,\tau} = \frac{k_3}{k_2^{3/2}} = \frac{A_3 + B_3 v_t + C_3 \lambda_t^{\mathbb{Q}}}{\left(A_2 + B_2 v_t + C_2 \lambda_t^{\mathbb{Q}}\right)^{3/2}}. \quad (10)$$

Similar formulas can be obtained for the SVCJ and SVCJI models by using the corresponding MGF given in Appendix A.2.

We use central finite differences to approximate A_2, B_2, C_2, A_3, B_3 and C_3 with the spacing of 0.01 for ω . For example, A_2 and A_3 can be approximated as

$$A_2 = \frac{\partial^2 A(\omega, \tau)}{\partial \omega^2} \Big|_{\omega=0} \approx \frac{A(-d, \tau) + A(d, \tau)}{d^2},$$

$$A_3 = \frac{\partial^3 A(\omega, \tau)}{\partial \omega^3} \Big|_{\omega=0} \approx \frac{-\frac{1}{2}A(-2d, \tau) + A(-d, \tau) - A(d, \tau) + \frac{1}{2}A(2d, \tau)}{d^3},$$

where $d = 0.01$. Given $\tau = 30/365$, $A(-0.02, \tau)$, $A(-0.01, \tau)$, $A(0.01, \tau)$ and $A(0.02, \tau)$ can be easily calculated from Equations (26)–(28) in Appendix A.2.

3. Data

3.1 S&P 500 and CBOE indices

The S&P 500 Index (SPX) is downloaded from Bloomberg and the CBOE indices are obtained from the CBOE. Throughout this paper, we use the converted (actual) value for CBOE indices. In detail, the VIX is divided by 100 and the SKEW is taking the difference between 100 and the CBOE SKEW and then divided by 10. This paper mainly focuses on the risk-neutral information extracted from the one-month VIX (VIX30), the one-year VIX (VIX365) and the one-month SKEW. For the VIX30, we directly use the CBOE VIX, while for the VIX365, we calculate from option data as the VIX term structure data are available after 24

November 2010. In order to improve the computing accuracy, for each maturity, we interpolate implied volatilities using a cubic spline across moneyness levels to obtain a continuum of implied volatilities. For moneyness levels above or below the available moneyness level in the market, we use the implied volatility of the highest or lowest available strike price. After implementing this interpolation-extrapolation technique, we get a fine grid of one thousand implied volatilities for moneyness levels between 0.01% and 300%. Using the Black–Scholes formula, we then convert the implied volatilities into the corresponding option prices. Given these option prices, we apply the CBOE method given in the CBOE VIX white paper to compute the near-term and far-term VIX365. Linear interpolation between maturities is used to calculate the moments at a fixed 365-day horizon. Option data are obtained from Ivy DB database provided by OptionMetrics.

All indices are from 02 January 1996 to 29 April 2016, which are consistent with the option data period. In order to study the out-of-sample pricing performance, we divide the sample into two subsamples: 02 January 1996 – 31 December 2014 (in-sample) and 02 January 2015 – 29 April 2016 (out-of-sample). The descriptive statistics of the SPX, index returns, VIX30, VIX365 and SKEW are summarized in Table 3 and their time series are plotted in Figure 1.

Table 3: Descriptive statistics of the SPX, index returns, VIX30, VIX365 and SKEW. Data are from 02 January 1996 to 29 April 2016.

	1996-2014 (In-sample)					2015-2016 (Out-of-sample)				
	Mean	Std.dev.	Min.	Median	Max.	Mean	Std.dev.	Min.	Median	Max.
Index level (\$)	1220.27	291.81	598.48	1210.75	2090.57	2041.92	70.11	1829.08	2064.12	2130.82
Daily return (%)	0.0251	1.2463	-9.4695	0.0678	10.9572	0.0009	0.9949	-4.0211	-0.0159	3.8291
VIX30 (%)	21.21	8.42	9.89	19.73	80.86	17.22	4.49	11.95	15.62	40.74
VIX365 (%)	23.03	6.00	22.56	13.45	54.09	21.54	2.05	21.07	18.31	27.56
SKEW	-1.83	0.62	-4.62	-1.78	-0.41	-2.73	0.68	-4.65	-2.58	-1.38

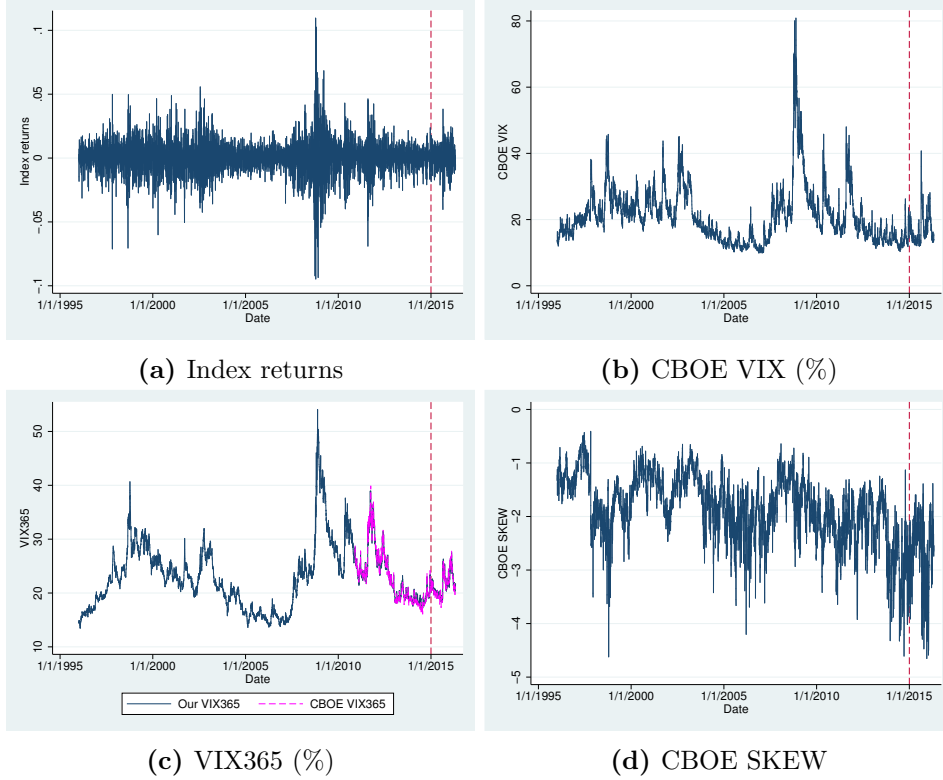


Figure 1: Time series of the SPX, index returns, VIX30, VIX365 and CBOE SKEW. Data are from 02 January 1996 to 29 April 2016.

Table 3 shows that the standard deviation of the daily return is 1.2463% during the in-sample period, which can be converted to annualized standard deviation, $1.2463\% \times \sqrt{252} = 19.7844\%$. Furthermore, the average daily return of the SPX is 0.0251% from 1996 to 2014, while the average daily return decreases to 0.0009% from 2015 to 2016. The more recent data of the SPX have a lower average daily return. Similarly, the average VIX30 decreases from 21.21% (1996–2014) to 17.22% (2015–2016). For the in-sample VIX data, the average VIX365 is higher than the average VIX30. This leads to the term structure of the VIX. Figure 1b and Figure 1c plot the dynamics of the VIX30 and VIX365, respectively. Roughly speaking, the peaks occur during the periods of financial crises. For example, the maximum of the VIX30, 80.86%, is on 20 November 2008 (i.e., Financial crisis of 2008). Based on the minimum and maximum of the SKEW, we find that the SKEW is always negative from 1996 to 2016. This is verified by the time series of the SKEW in Figure 1d. The average SKEW during the out-of-sample period is -2.73 , which is more negative than the average

SKEW during the in-sample period. On 20 November 2008, the VIX30 sharply peaks to the maximum, while the value of the SKEW is only -1.493 . This indicates that the VIX and SKEW seem to delivery different information in the financial market.

Table 4: Our VIX365 v.s. CBOE VIX365. Data are from 24 November 2010 to 30 April 2016.

	Mean	Std.dev.	Min.	Median	Max.	Corr.
CBOE VIX365	22.56	4.39	21.46	16.05	39.91	1.00
Our VIX365	22.55	4.21	21.49	16.66	38.95	

Additionally, a comparison of our VIX365 and the CBOE VIX365 is given in Table 4. As the VIX term structure data are available only after 24 November 2010, we calculate the VIX365 from option data by using the interpolation-extrapolation technique. For the period from 24 November 2010 to 30 April 2016, our VIX365 and the CBOE VIX365 have very close descriptive statistics and their correlation reaches 1.00. Their time series given in Figure 1c document that our VIX365 can dynamically match the CBOE VIX365 very well. This comparison highlights the accuracy of our VIX365, compared with the CBOE VIX365.

3.2 Options

Option data are obtained from Ivy DB database provided by OptionMetrics. Firstly, we filter out options whose prices are less than $3/8$ or violate arbitrage bounds, or the bid prices are zero or higher than its ask prices. Secondly, we only keep options with nonzero vega and nonzero trading volume. Thirdly, we keep options with days to maturity (DTM) between 7 and 365 days and moneyness (F/K) between 0.9 to 1.1, where K is strike price and the forward price $F = e^{(r-q)\tau}S$. Fourthly, we only keep the sample if the computed implied volatility is less than 5% differ to the implied volatility from the Ivy DB database. Finally, we use the Wednesday call and put index options in order to avoid weekend effects. After filtering, 147,203 options are left from 1996 to 2014, and 61,262 options are left from 2015 to 2016. Number of option contracts, option prices and implied volatility by maturity and moneyness are given in Table 5.

Table 5: Number of option contracts, option prices and implied volatility by maturity and moneyness. Option data are obtained from Ivy DB database provided by OptionMetrics and the sample period is from 02 January 1996 to 29 April 2016.

(F/K)\DTM	1996-2014 (In-sample, 147,203 options)					2015-2016 (Out-of-sample, 61,262 options)					
	≤ 30	30-90	90-180	180-250	> 250	≤ 30	30-90	90-180	180-250	> 250	
Panel A: Number of option contracts											
≤ 0.96	2830	17446	5450	2012	2117	≤ 0.96	2344	7587	1661	297	444
0.96-0.98	3286	10203	2527	899	977	0.96-0.98	2825	3871	564	107	158
0.98-1.02	8176	26110	6655	2372	2472	0.98-1.02	7177	8588	1553	351	490
1.02-1.04	3223	9571	2389	997	1050	1.02-1.04	3071	3200	485	102	166
1.04-1.06	2737	7849	2062	818	871	1.04-1.06	2499	2964	439	113	102
> 1.06	3877	12172	3321	1376	1358	> 1.06	3749	5190	774	167	224
Panel B: Average option prices											
≤ 0.96	13.83	18.96	33.81	49.54	59.88	≤ 0.96	26.96	16.47	29.23	52.62	83.25
0.96-0.98	14.96	26.60	47.99	67.99	81.10	0.96-0.98	23.04	31.94	59.28	89.46	118.76
0.98-1.02	21.77	33.08	54.05	72.68	88.39	0.98-1.02	29.36	46.28	73.48	102.21	126.40
1.02-1.04	24.33	33.99	52.64	68.98	83.79	1.02-1.04	35.88	45.37	75.40	101.97	126.65
1.04-1.06	23.90	32.26	51.21	63.99	79.80	1.04-1.06	35.52	37.17	66.80	98.68	109.13
> 1.06	18.57	27.59	46.01	60.40	71.74	> 1.06	25.50	26.99	56.63	86.08	99.03
Panel C: Average option implied volatility (%)											
≤ 0.96	17.57	16.56	16.66	17.46	17.92	≤ 0.96	14.89	12.11	12.01	13.80	14.99
0.96-0.98	14.21	15.99	17.60	18.55	18.97	0.96-0.98	12.86	13.04	14.69	15.93	16.95
0.98-1.02	15.34	17.39	18.55	19.23	19.47	0.98-1.02	15.07	15.60	16.46	16.80	17.47
1.02-1.04	17.89	19.31	19.81	19.78	19.60	1.02-1.04	17.96	17.84	18.09	18.17	18.72
1.04-1.06	19.95	20.55	20.49	20.57	20.39	1.04-1.06	19.86	19.21	19.12	18.63	19.00
> 1.06	22.98	22.47	21.69	21.61	21.11	> 1.06	22.75	21.02	20.29	20.20	20.48

From Panel A, Table 5, we find that at-the-money (ATM) options are the most popular. For example, for the in-sample period, the total number of ATM option contracts are 45,785, which is around one third of the total data sample. Furthermore, more than half of option contracts are with DTM between 30 to 90 days. Panel B, Table 5 gives the average option prices varying from 13.83 to 126.65. Panel C, Table 5 shows the average Black–Scholes implied volatility by maturity and moneyness. It straightforwardly describes the implied volatility surface. For example, during 1996 to 2014, the average implied volatility from the short-term options (i.e., $DTM \leq 30$) has a very steep U-shape smirk with a slope of 8.77 ($= 22.98 - 14.21$). The shape of the average implied volatility from the long-term options (i.e., $DTM \geq 250$) is flatter, with a slope of 3.19 ($= 21.11 - 17.92$). The average implied volatility for the in-sample options is 18.37%, which is quite close to the annualized volatility of the SPX returns (19.78%).

4. Estimation method

Following Eraker (2004); Kaeck and Alexander (2012); Yang and Kannianen (2017) and others, we use the Markov Chain Monte Carlo (MCMC) method to simultaneously estimate parameters in both physical and risk-neutral measures and the latent variables. We use the SVCJH model as an example to demonstrate the discretization of our model. First, we give the discretized process by using the Euler scheme,

$$\begin{cases} \log S_{t+h} - \log S_t = (r - q + \phi_t - \frac{1}{2}v_t - \lambda_t m) h + \sqrt{v_t h} \varepsilon_{t,S} + x_t b_t, \\ v_{t+h} = v_t + \kappa (\theta - v_t) h + \sigma_v \sqrt{v_t h} \varepsilon_{t,v} + y_t b_t, \\ \lambda_{t+h} = \lambda_t + \beta (\lambda_\infty - \lambda_t) h + z_t b_t, \end{cases} \quad (11)$$

where $h = 1/252$, $\phi_t = \eta^S v_t + \lambda_t m - \lambda_t^{\mathbb{Q}} m^{\mathbb{Q}}$, $\varepsilon_{t,S}, \varepsilon_{t,v} \sim N(0, 1)$, $Corr(\varepsilon_{t,S}, \varepsilon_{t,v}) = \rho$, $x_t \sim N(\mu_x, \sigma_x^2)$, $y_t \sim Exp(1/\mu_y)$, $z_t \sim Exp(1/\mu_z)$, $b_t \sim Bernoulli(\lambda_t h)$. Furthermore, we consider the CBOE indices as additional inputs,

$$\log I_{t,\tau}^{\text{Market}} = \log I_{t,\tau}^{\text{Model}} + \varepsilon_t, \quad \varepsilon_{t+1} \sim N(\rho_\varepsilon \varepsilon_t, \sigma_\varepsilon^2), \quad (12)$$

where inputs I_t can be $VIX_{t,30}^2$, $\{VIX_{t,30}^2, -SKEW_{t,30}\}$ or $\{VIX_{t,30}^2, VIX_{t,360}^2\}$. As the SKEW is always negative, we use positive value of the SKEW as inputs, in order to guarantee the pricing errors being log-normal following Eraker (2004); Kaeck and Alexander (2012) and Yang and Kannianen (2017).

Denote $\Theta = \{\eta^S, \mu_x, \sigma_x, \kappa, \theta, \sigma_v, \rho, \mu_y, \beta, \lambda_\infty, \mu_z, \mu_x^{\mathbb{Q}}, \kappa^{\mathbb{Q}}, \mu_y^{\mathbb{Q}}, \eta^\lambda, \rho_\varepsilon, \sigma_\varepsilon\}$ as the parameter set that we want to estimate. Denote $\mathbf{S} = S_t|_{t=0}^{t=T}$, $\mathbf{I} = I_t|_{t=0}^{t=T}$ as the observed data and $\mathcal{D} = \{S_t, I_t\}$. Denote $\mathbf{v} = v_t|_{t=0}^{t=T}$ and $\boldsymbol{\lambda} = \lambda_t|_{t=0}^{t=T}$ as the hidden state variables.⁴ Then the posterior distribution function can be expressed as

$$\begin{aligned} p(\Theta, \mathbf{v}, \boldsymbol{\lambda} | \mathcal{D}) &\propto p(\Theta, \mathbf{v}, \boldsymbol{\lambda}, \mathcal{D}) \propto p(\mathcal{D} | \Theta, \mathbf{v}, \boldsymbol{\lambda}) p(\Theta, \mathbf{v}, \boldsymbol{\lambda}) \\ &\propto p(\mathcal{D} | \Theta, \mathbf{v}, \boldsymbol{\lambda}) p(\mathbf{v}, \boldsymbol{\lambda} | \Theta) p(\Theta). \end{aligned}$$

If we assume conditional independence among the observed data, we can further simplify the

⁴Actually, $\varepsilon_t|_{t=0}^{t=T}$ is also a hidden state variable.

previous expression as

$$\begin{aligned}
p(\Theta, \mathbf{v}, \boldsymbol{\lambda}|\mathcal{D}) &\propto p(\mathcal{D}|\Theta, \mathbf{v}, \boldsymbol{\lambda})p(\mathbf{v}, \boldsymbol{\lambda}|\Theta)p(\Theta) \\
&\propto p(\mathbf{S}|\Theta, \mathbf{v}, \boldsymbol{\lambda})p(\mathbf{VIX}|\Theta, \mathbf{v}, \boldsymbol{\lambda})p(\mathbf{v}, \boldsymbol{\lambda}|\Theta)p(\Theta) \\
&\propto \prod_{t=1}^T p(S_t|\Theta, v_t, \lambda_t) \prod_{t=1}^T p(I_t|\Theta, v_t, \lambda_t)p(\mathbf{v}, \boldsymbol{\lambda}|\Theta)p(\Theta).
\end{aligned}$$

We can use further simplify $p(\mathbf{v}, \boldsymbol{\lambda}|\Theta)$ using filter method. Notice that

$$p(v_t, v_{t-1}, \lambda_t, \lambda_{t-1}|\Theta) \propto p(v_t, \lambda_t|v_{t-1}, \lambda_{t-1}, \Theta)p(v_{t-1}, \lambda_{t-1}|\Theta)$$

and

$$p(v_t, \lambda_t|v_{t-1}, \lambda_{t-1}, \Theta) \propto p(v_t|\lambda_t, v_{t-1}, \Theta)p(\lambda_t|\lambda_{t-1}, \Theta).$$

So the term $p(\mathbf{v}, \boldsymbol{\lambda}|\Theta)$ can be rewritten as

$$\begin{aligned}
p(\mathbf{v}, \boldsymbol{\lambda}|\Theta) &\propto p(v_0, \lambda_0|\Theta) \prod_{t=1}^T p(v_t, \lambda_t|v_{t-1}, \lambda_{t-1}, \Theta) \\
&\propto p(v_0, \lambda_0|\Theta) \prod_{t=1}^T p(v_t|\lambda_t, v_{t-1}, \Theta)p(\lambda_t|\lambda_{t-1}, \Theta).
\end{aligned}$$

Therefore, the posterior distribution function can be divided into smaller pieces as

$$\begin{aligned}
p(\Theta, \mathbf{v}, \boldsymbol{\lambda}|\mathcal{D}) & \\
&\propto p(v_0, \lambda_0|\Theta)p(\Theta) \prod_{t=1}^T p(S_t|\Theta, v_t, \lambda_t)p(I_t|\Theta, v_t, \lambda_t)p(v_t|\lambda_t, v_{t-1}, \Theta)p(\lambda_t|\lambda_{t-1}, \Theta) \\
&\propto p(v_0, \lambda_0, \Theta) \prod_{t=1}^T p(S_t|\Theta, v_t, \lambda_t)p(I_t|\Theta, v_t, \lambda_t)p(v_t|\lambda_t, v_{t-1}, \Theta)p(\lambda_t|\lambda_{t-1}, \Theta).
\end{aligned}$$

Hence, in order to use the posterior distribution, we need to specify the prior distribution $p(v_0, \lambda_0, \Theta)$ and use the MCMC method to sample the posterior distribution. We choose prior distribution $p(v_0, \lambda_0, \Theta)$ that is identical to the one in Eraker et al. (2003) or use a similarly uninformative distribution according to Johannes and Polson (2009).

5. Empirical results

5.1 Parameter estimation and goodness of fit

Denote the observed data sets as $\mathcal{D}_0 = \{S_t, VIX_{t,30}^2\}$, $\mathcal{D}_1 = \{S_t, VIX_{t,30}^2, VIX_{t,365}^2\}$ and $\mathcal{D}_2 = \{S_t, VIX_{t,30}^2, -SKEW_{t,30}\}$. For each data set, we run the MCMC algorithm for 100,000 iterations, discarding the first 10,000 as a burn-in-period to achieve the convergence of the chain. Additionally, in order to study the goodness of fit of the models, we calculate the Deviance Information Criterion (DIC) for each model. The explicit expression of the DIC can be found in Appendix C in Yang and Kannianen (2017). The DIC uses log-likelihoods to measure goodness of fit. A lower DIC indicates that a model has better goodness of fit. Table 6 gives the parameter estimates using different data sets.

The parameter estimates vary across different models and data sets. The price jump size μ_x varies from -0.0150 to -0.608 and its volatility σ_x varies from 0.0178 to 0.0451 . The annualized jump mean in volatility reaches around 5%. The jump intensity for the SVCJ model is 1.0349 using \mathcal{D}_0 , 0.4626 using \mathcal{D}_1 and 1.1264 using \mathcal{D}_2 . In other words, jumps occur once a year or two years. Our jump parameters are consistent with Eraker et al. (2003); Eraker (2004); Zhu and Lian (2012); Kaeck and Alexander (2012). In line with Egloff, Leippold, and Wu (2010); Kaeck and Alexander (2012); Bardgett et al. (2018), the correlation estimate, ρ , is around -0.8 . The equity premium contributed from the volatility η^S varies from -0.0552 to -0.2446 . The negative sign is consistent with Du and Luo (2017). According to the equilibrium model in Ruan and Zhang (2018), η^S should be positive. Actually η^S estimates are very noisy with large standard deviations (which are almost the same as the absolute values of the estimates). In line with Du and Luo (2017), η^S is difficult to be estimated.

Most of the diffusive volatility risk premiums, $\eta^v = \kappa^{\mathbb{Q}} - \kappa$, are positive in our calibrations varying from 0.2245 to 8.9144 , except for the SVCJI model using \mathcal{D}_1 . This strongly supports the negative variance risk premium in the empirical VIX and variance swaps literature, e.g., Egloff et al. (2010); Bardgett et al. (2018). Consistent with the equilibrium model in Ruan and Zhang (2018), the price jump risk premium $\eta^x = \mu_x - \mu_x^{\mathbb{Q}}$ and the volatility jump risk premium $\eta^y = \mu_y^{\mathbb{Q}} - \mu_y$ are all positive and the jump intensity risk premium $\eta^\lambda = \lambda_t^{\mathbb{Q}}/\lambda_t > 1$. In other words, jumps contribute very large part of the negative variance risk premium, e.g.,

Todorov (2010); Bollerslev and Todorov (2011); Li and Zinna (2018).

Table 6: Parameter estimates using different data sets. Data are from 02 January 1996 to 31 December 2014. We discard the first 10,000 runs as a “burn-in” period and use the last 100,000 iterations in MCMC simulations to estimate model parameters. For each parameter to be estimated, we use the similar priors, that is identical to Eraker et al. (2003) or use a similarly uninformative distribution according to Johannes and Polson (2009). Specifically, we take the mean of the posterior distribution as the parameter estimate and the standard deviation of the posterior as the standard error in parentheses.

η^S	μ_x	σ_x	κ	θ	σ_v	ρ	μ_H	(β)	$\lambda_1 (\lambda_\infty)$	$\lambda_2 (\mu_z)$	μ_x^Q	κ^Q	μ_H^Q	η^λ	DIC
Panel A: Parameter Estimates using \mathcal{D}_0 (benchmark)															
SVCJ Model															
-0.1861 (0.1787)	-0.0374 (0.0038)	0.0267 (0.0035)	5.0043 (0.4612)	0.0084 (0.0010)	0.4796 (0.0004)	-0.7718 (0.0065)	0.0501 (0.0058)		1.0349 (0.0504)		-0.0659 (0.0008)	1.0181 (0.0179)	0.0501 (0.0058)	1.0177 (0.0201)	-65140
SVCJI Model															
-0.1666 (0.1625)	-0.0390 (0.0077)	0.0574 (0.0238)	5.8089 (0.4814)	0.0092 (0.0007)	0.4488 (0.0079)	-0.7886 (0.0060)	0.0405 (0.0048)		0.3563 (0.0355)	23.6781 (2.5290)	-0.0852 (0.0085)	3.8548 (0.4926)	0.0746 (0.0228)	1.1104 (0.0521)	-67080
SVCJH Model															
-0.1775 (0.1731)	-0.0328 (0.0053)	0.0179 (0.0045)	9.9404 (0.0576)	0.0195 (0.0003)	0.4996 (0.0004)	-0.7302 (0.0078)	0.0463 (0.0083)	5.5258 (0.4846)	0.0502 (0.0002)	4.7808 (0.1702)	-0.2020 (0.0096)	1.0260 (0.0257)	0.2931 (0.0076)	1.0711 (0.0493)	-71460
Panel B: Parameter Estimates using \mathcal{D}_1 .															
SVCJ Model															
-0.2446 (0.2265)	-0.0608 (0.0093)	0.0338 (0.0092)	3.0140 (0.2896)	0.0207 (0.0021)	0.4784 (0.0016)	-0.8430 (0.0119)	0.0675 (0.0190)		0.4626 (0.0630)		-0.1018 (0.0131)	1.6324 (0.0271)	0.0727 (0.0028)	1.0618 (0.0654)	-67118
SVCJI Model															
-0.0552 (0.0541)	-0.0321 (0.0035)	0.0274 (0.0019)	4.8301 (0.0264)	0.0124 (0.0005)	0.3824 (0.0070)	-0.8645 (0.0049)	0.0279 (0.0029)		0.1191 (0.0308)	43.9284 (4.0979)	-0.0282 (0.0074)	5.1670 (0.0241)	0.0885 (0.0034)	1.0254 (0.0100)	-70405
SVCJH Model															
-0.1427 (0.1379)	-0.0573 (0.0063)	0.0451 (0.0058)	3.0242 (0.0242)	0.0083 (0.0007)	0.4995 (0.0007)	-0.8166 (0.0050)	0.0571 (0.0059)	3.0061 (0.0059)	0.0503 (0.0004)	4.1319 (0.5300)	-0.0573 (0.0063)	2.7997 (0.0003)	0.0751 (0.0053)	1.1643 (0.0920)	-84022
Panel C: Parameter Estimates using \mathcal{D}_2															
SVCJ Model															
-0.1440 (0.1434)	-0.0453 (0.0053)	0.0415 (0.0033)	3.3845 (0.3726)	0.0138 (0.0017)	0.5759 (0.0201)	-0.9153 (0.0026)	0.0464 (0.0058)		1.1264 (0.1089)		-0.0593 (0.0040)	1.0191 (0.0204)	0.0464 (0.0058)	1.0197 (0.0194)	-66748
SVCJI Model															
-0.7103 (0.2384)	-0.0150 (0.0004)	0.0178 (0.0019)	3.3064 (0.4831)	0.0158 (0.0021)	0.3269 (0.0099)	-0.5948 (0.0221)	0.0083 (0.0019)		0.2201 (0.0286)	36.9487 (3.7363)	-0.0358 (0.0049)	2.0683 (0.6949)	0.2437 (0.0049)	1.0301 (0.0258)	-69141
SVCJH Model															
-0.2090 (0.1910)	-0.0352 (0.0078)	0.0305 (0.0363)	9.9294 (0.1729)	0.0206 (0.0004)	0.4989 (0.0078)	-0.7135 (0.0112)	0.0466 (0.0088)	4.9662 (1.3903)	0.0501 (0.0012)	4.9037 (0.0907)	-0.1913 (0.0162)	1.0580 (0.0524)	0.2950 (0.0253)	1.1933 (0.0927)	-82324

According to DIC values, we find that the SVCJH model outperforms among three typical models using different data sets. Furthermore, in order to separately get the matching performance for the three CBOE indices, following Equation (12), we compute the root mean square errors (RMSE) of inputs as

$$RMSE_I = 100\% \times \sqrt{\frac{1}{N} \sum_t \left(\log(\hat{I}_t) - \log(I_t) \right)^2}, \quad (13)$$

where I_t is the market data and \hat{I}_t is calculated based on the model. I_t can be $VIX_{t,30}^2$, $VIX_{t,365}^2$ and $-SKEW_{t,30}$.

Table 7: RMSE of $VIX_{t,30}^2$, $VIX_{t,365}^2$ and $-SKEW_{t,30}$. The RMSEs of CBOE indices that are not as inputs for the calibration are given in parentheses. Data are from 02 January 1996 to 31 December 2014.

	VIX30			VIX365			SKEW		
	SVCJ	SVCJI	SVCJH	SVCJ	SVCJI	SVCJH	SVCJ	SVCJI	SVCJH
\mathcal{D}_0	12.30	2.26	1.63	(42.30)	(30.03)	(95.89)	(67.10)	(46.42)	(14.98)
\mathcal{D}_1	9.63	37.22	2.03	29.49	14.30	3.92	(62.79)	(67.83)	(47.49)
\mathcal{D}_2	10.55	49.16	2.09	(53.40)	(513.05)	(110.60)	49.01	23.02	11.02

All RMSEs are given in Table 7.⁵ The RMSEs of CBOE indices that are not as inputs for the calibration are given in parentheses. Table 7 actually reveals two important hypotheses.

- (i) If the VIX30 can capture well the short-term option information, then estimated by using different data sets (i.e., $\mathcal{D}_0, \mathcal{D}_1$ and \mathcal{D}_2), the SVCJH model will outperform in terms of pricing short-term options (i.e., $DTM \leq 30$);
- (ii) If the VIX30 and the VIX365 can capture well the option volatility surface, then SVCJH model will outperform in terms of pricing options (e.g., the SVCJH estimated by using \mathcal{D}_1 will be better than the SVCJI estimated by using \mathcal{D}_0).

The first hypothesis is due to the fact that the SVCJH model has the lowest RMSE among three models estimated by using different data sets. Estimated by using \mathcal{D}_0 , the RMSEs of the VIX30 and VIX365 under the SVCJI are 2.26% and 30.03%, respectively. After adding the VIX365, the RMSEs of the VIX30 and VIX365 under the SVCJH are 2.03% and 3.92%, respectively. If the VIX30 and the VIX365 can capture well the option volatility surface, according to their RMSEs, then SVCJH model should outperform in terms of pricing options. Finally, through comparing option pricing performance, we can verify the following three hypotheses.

- (iii) If the VIX365 is informative for option prices, adding the VIX365 can increase all models' option pricing performance;

⁵Time series of the model-implied CBOE indices are given in Appendix C.

- (iv) If the SKEW is informative for option prices, adding the SKEW can increase all models' option pricing performance;
- (v) If the VIX365 is more informative than the SKEW for option prices, models' option pricing performance using \mathcal{D}_1 will be overall better than using \mathcal{D}_2 .

5.2 Option pricing performance

In order to test the above five hypotheses, in this section, we investigate the option pricing performance under different models estimated by using different data sets. First of all, in line with Kaeck and Alexander (2012); Yang and Kannianen (2017), we compute the root mean square errors scaled by the Black–Scholes vegas ($\mathcal{V}RMSEs$) as

$$\mathcal{V}RMSE = 100 \times \sqrt{\frac{1}{N} \sum_{t,i} \left(\frac{\widehat{c}(T_{t,i}, K_{t,i}) - c(T_{t,i}, K_{t,i})}{\mathcal{V}(T_{t,i}, K_{t,i})} \right)^2}, \quad (14)$$

where $c(T_{t,i}, K_{t,i})$ is the market option price at time t for particular maturity $T_{t,i}$ and strike price $K_{t,i}$; $\widehat{c}(T_{t,i}, K_{t,i})$ is the model-implied price and $\mathcal{V}(T_{t,i}, K_{t,i})$ is the Black–Scholes vega; N is the total number of options during the corresponding sample period. The model-implied prices are calculated by using the fast Fourier transform (FFT) in Carr and Madan (1999), see Appendix A.3.

5.2.1 In-sample performance

Following Equation (14), we calculate the $\mathcal{V}RMSEs$ by moneyness and maturity using the information from the SPX and CBOE indices during the in-sample period from 1996 to 2014. The results are given in Table 8.

Table 8: In-sample \mathcal{V} RMSEs by moneyness and maturity using the information from S&P 500 and VIX30 indices. Data are from 02 January 1996 to 31 December 2014.

	\mathcal{D}_0			\mathcal{D}_1			\mathcal{D}_2		
	SVCJ	SVCJI	SVCJH	SVCJ	SVCJI	SVCJH	SVCJ	SVCJI	SVCJH
Panel A: Overall	2.94	2.02	4.40	2.54	3.31	2.53	2.84	7.08	4.72
Panel B: Sorting by moneyness									
≤ 0.96	4.07	2.84	5.73	3.67	5.01	3.72	3.42	9.54	6.19
0.96-0.98	2.93	2.11	4.35	2.62	3.50	2.80	2.61	6.51	4.65
0.98-1.02	2.53	1.65	3.98	2.14	2.87	2.23	2.42	6.12	4.27
1.02-1.04	2.54	1.52	3.93	2.03	2.45	1.89	2.76	6.15	4.19
1.04-1.06	2.47	1.65	3.82	1.98	2.25	1.73	2.85	6.27	4.09
> 1.06	2.40	1.88	3.86	1.95	2.04	1.62	3.01	6.62	4.14
Panel C: Sorting by time to maturity									
≤ 30	3.12	2.10	1.77	2.90	4.16	2.55	2.61	4.16	1.75
30-90	2.85	1.93	2.89	2.59	3.59	2.18	2.65	5.94	3.02
90-180	2.61	1.97	5.37	2.03	1.90	2.53	2.81	10.89	5.84
180-250	3.11	2.26	7.91	2.14	1.47	3.48	3.48	9.65	8.85
> 250	3.69	2.52	10.11	2.44	1.61	4.05	4.21	7.99	10.74

First, comparing \mathcal{V} RMSEs of short-term options (i.e., $\text{DTM} \leq 30$), we indeed find that the SVCJH model has the lowest \mathcal{V} RMSEs across different data sets (i.e., $\mathcal{D}_0, \mathcal{D}_1$ and \mathcal{D}_2). It seems that the VIX30 indeed provides very informative short-term option information. Second, the overall \mathcal{V} RMSE of the SVCJH estimated by using \mathcal{D}_1 is larger than the overall \mathcal{V} RMSE of the SVCJI estimated by using \mathcal{D}_0 , i.e., 2.53% v.s. 2.02%. This shows that the VIX30 and VIX365 may not capture well the option volatility surface. This may be caused by the definition of the VIX, that is the aggregate volatility across different moneyness. Furthermore, the inconsistency may be also due to the calculation errors, e.g., Liu and van der Heijden (2016). The VIX is not the same as the Black-Scholes implied volatility. Third, comparing \mathcal{V} RMSEs using \mathcal{D}_0 and \mathcal{D}_1 , there is a big decrease in the SVCJ and SVCJH models, however, the SVCJI model has larger \mathcal{V} RMSEs after adding VIX365. The answer of whether the VIX365 is informative for option prices depends on the model we choose. Actually, the SVCJI model estimated by using only the SPX and VIX30 works best among three models and three data sets. Fourth, comparing \mathcal{V} RMSEs using \mathcal{D}_0 and \mathcal{D}_2 , adding the SKEW can significantly increase \mathcal{V} RMSEs for the SVCJI and SVCJH models. The SVCJ model almost does not change. Roughly speaking, the SKEW is very noisy index for option prices. This is consistent with Liu and van der Heijden (2016) who find that the estimation errors of true skewness by using the CBOE SKEW method are very large. Finally, comparing

\mathcal{V} RMSEs using \mathcal{D}_1 and \mathcal{D}_2 , we conclude that VIX365 is more informative than SKEW for option prices.

5.2.2 Out-of-sample performance

For the out-of-sample performance assessment, given the parameter estimates calibrated for the period from 1996 to 2014, we need to filter out the unobservable latent state variables v_t and λ_t . Following Kaeck and Alexander (2012), we fix the model parameters from the in-sample estimation and input the market data in order to obtain draws from the MCMC procedure. Using the out-of-sample latent state variables v_t and λ_t and the model parameters from the in-sample estimation, we calculate the option prices by using the fast Fourier transform (FFT) in Carr and Madan (1999) and compute the \mathcal{V} RMSEs following Equation (14). The out-of-sample \mathcal{V} RMSEs are presented in Table 9.

Table 9: Out-of-sample \mathcal{V} RMSEs by moneyness and maturity using the information from S&P 500 and VIX30 indices. Data are from 02 January 2015 to 29 April 2016.

	\mathcal{D}_0			\mathcal{D}_1			\mathcal{D}_2		
	SVCJ	SVCJI	SVCJH	SVCJ	SVCJI	SVCJH	SVCJ	SVCJI	SVCJH
Panel A: Overall	3.96	1.82	3.67	2.61	3.00	2.35	2.34	6.04	3.96
Panel B: Sorting by moneyness									
≤ 0.96	6.90	2.63	6.08	4.33	4.99	3.69	3.32	9.08	6.58
0.96-0.98	3.75	1.67	3.44	2.68	3.51	2.47	2.32	5.06	3.66
0.98-1.02	2.79	1.23	2.89	1.85	2.21	1.79	1.82	5.36	3.10
1.02-1.04	2.46	1.29	2.47	1.63	1.80	1.60	1.87	5.07	2.66
1.04-1.06	2.63	1.94	2.38	2.00	1.88	1.92	2.32	4.68	2.54
> 1.06	2.06	1.85	2.28	1.63	1.38	1.62	2.00	4.30	2.45
Panel C: Sorting by time to maturity									
≤ 30	3.96	2.13	1.68	2.74	3.49	2.57	2.27	5.10	1.72
30-90	4.02	1.69	3.11	2.63	2.92	2.11	2.24	5.86	3.34
90-180	3.83	1.50	6.20	2.26	1.85	2.16	2.54	9.24	6.80
180-250	3.49	1.09	8.33	1.84	1.03	3.08	2.94	7.41	9.20
> 250	3.64	0.88	10.40	1.81	0.91	3.53	3.61	6.26	11.11

Compared with Table 8, there are two new messages obtained in Table 9. First, Panel C, Table 9 shows that the SVCJI model works very well in terms of pricing long-term options (i.e., $\text{DTM} > 250$) even calibrated by using the SPX and VIX30 only (i.e., \mathcal{D}_0). Second, overall, for all models and data sets, the out-of-sample option pricing performance is better than the in-sample option pricing performance.

5.3 Volatility smirk

Following Yang and Kannianen (2017), we also calculate the implied volatility root mean square errors (IVRMSEs) as

$$IVRMSE = 100 \times \sqrt{\frac{1}{N} \sum_{t,i} (\hat{\sigma}_{BS}(T_{t,i}, K_{t,i}) - \sigma_{BS}(T_{t,i}, K_{t,i}))^2}, \quad (15)$$

where $\sigma_{BS}(T_{t,i}, K_{t,i})$ is the Black–Scholes implied volatility based on the market price of the option at time t for particular maturity $T_{t,i}$ and strike price $K_{t,i}$; $\hat{\sigma}_{BS}(T_{t,i}, K_{t,i})$ is the Black–Scholes implied volatility based on the model price of the option. The IVRMSEs for the in-sample period are given in Table 10 and the IVRMSEs for the out-of-sample period are given in Table 11.

Table 10: In-sample IVRMSEs by moneyness and maturity using the information from SPX and CBOE indices. Data are from 02 January 1996 to 31 December 2014.

	\mathcal{D}_0			\mathcal{D}_1			\mathcal{D}_2		
	SVCJ	SVCJI	SVCJH	SVCJ	SVCJI	SVCJH	SVCJ	SVCJI	SVCJH
Panel A: Overall	2.70	1.94	4.16	2.35	2.90	2.44	2.69	6.38	4.46
Panel B: Sorting by moneyness									
≤ 0.96	3.45	2.69	5.03	3.24	3.85	3.53	3.18	7.50	5.41
0.96-0.98	2.80	2.12	4.22	2.54	3.29	2.75	2.60	6.17	4.52
0.98-1.02	2.48	1.63	3.95	2.09	2.79	2.19	2.38	6.03	4.23
1.02-1.04	2.44	1.47	3.87	1.95	2.35	1.83	2.64	6.00	4.13
1.04-1.06	2.33	1.54	3.72	1.85	2.13	1.66	2.66	6.00	3.97
> 1.06	2.25	1.70	3.68	1.78	1.99	1.55	2.72	6.10	3.94
Panel C: Sorting by time to maturity									
≤ 30	2.67	1.88	1.60	2.52	3.47	2.20	2.33	3.81	1.59
30-90	2.59	1.84	2.62	2.41	3.16	2.05	2.49	5.11	2.73
90-180	2.53	1.97	5.03	1.99	1.86	2.61	2.74	9.97	5.45
180-250	3.05	2.26	7.59	2.11	1.47	3.56	3.42	9.14	8.50
> 250	3.64	2.51	9.83	2.41	1.61	4.11	4.14	7.69	10.43

Table 11: Out-of-sample IVRMSEs by moneyness and maturity using the information from SPX and CBOE indices. Data are from 02 January 2015 to 29 April 2016.

	\mathcal{D}_0			\mathcal{D}_1			\mathcal{D}_2		
	SVCJ	SVCJI	SVCJH	SVCJ	SVCJI	SVCJH	SVCJ	SVCJI	SVCJH
Panel A: Overall	3.08	1.50	3.17	2.14	2.37	1.99	2.05	5.20	3.39
Panel B: Sorting by moneyness									
≤ 0.96	4.55	2.14	4.66	3.24	3.50	2.89	2.72	5.24	4.96
0.96-0.98	3.48	1.66	3.29	2.53	2.99	2.36	2.32	5.03	3.50
0.98-1.02	2.74	1.21	2.87	1.82	2.13	1.76	1.80	5.35	3.08
1.02-1.04	2.28	1.04	2.42	1.42	1.52	1.38	1.67	5.36	2.61
1.04-1.06	2.08	1.19	2.21	1.39	1.32	1.35	1.73	5.12	2.38
> 1.06	1.83	1.31	2.18	1.29	1.22	1.30	1.69	4.93	2.35
Panel C: Sorting by time to maturity									
≤ 30	2.84	1.59	1.51	2.11	2.72	1.95	1.82	5.46	1.57
30-90	3.12	1.48	2.48	2.19	2.30	1.81	1.99	4.76	2.62
90-180	3.49	1.43	5.13	2.12	1.58	2.19	2.40	5.94	5.56
180-250	3.36	1.08	7.85	1.79	1.01	3.14	2.88	6.72	8.66
> 250	3.57	0.88	10.07	1.79	0.91	3.58	3.56	5.97	10.74

Based on Broadie et al. (2007); Yang and Kannianen (2017), the IVRMSEs are identical to the \mathcal{V} RMSEs. Therefore, same conclusions are made in Tables 10 and 11. This also highlights the importance of the Black–Scholes implied volatility. Carr and Wu (2016) emphasize that institutional investors manage their volatility views and exchange their quotes not through option prices, but through the option implied volatility computed from the Black and Scholes (1973) model. In general, modelling option prices essentially is modelling the option implied volatility.

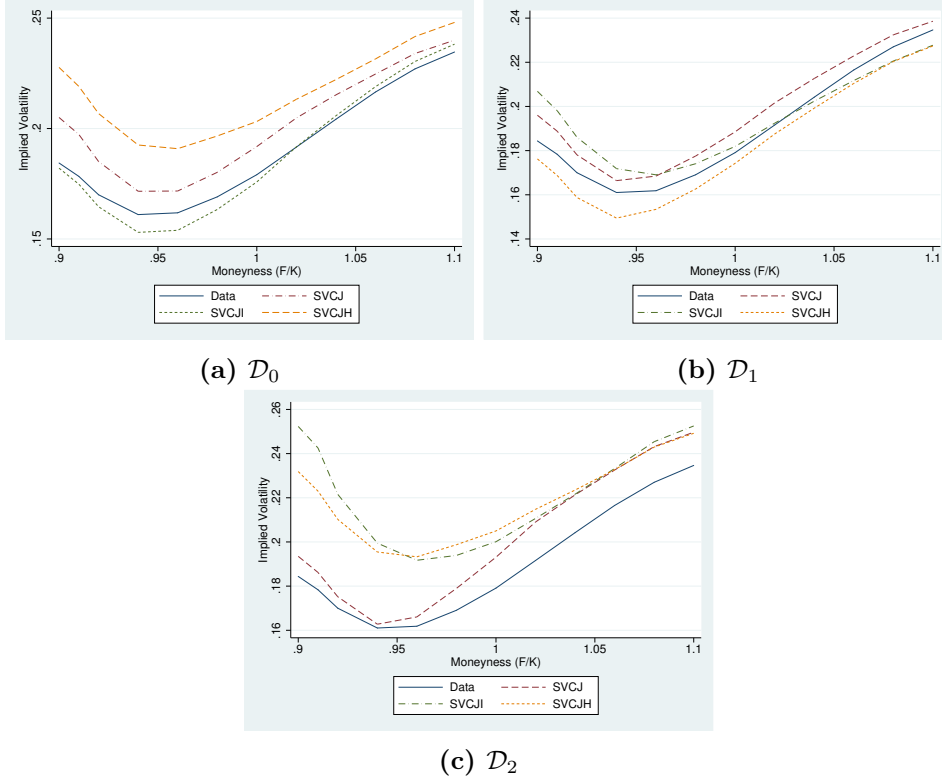


Figure 2: Average implied volatilities computed from the model option prices. The option sample is Wednesday options from 1996 to 2015.

Figure 2 plots the average implied volatilities against different moneyness. Roughly speaking, adding the VIX365 can significantly increase the goodness of fitting the implied volatility curves (comparing Figure 2a and Figure 2b), while adding the SKEW can decrease the goodness of fitting the implied curves (comparing Figure 2a and Figure 2c). The SVCJI model works best among three model when the model is calibrated by using \mathcal{D}_0 , while it works worst among three model when the model is calibrated by using \mathcal{D}_2 .

6. Conclusion

This study fills a notable gap in the current literature on inferring information from the SPX and CBOE indices for the option prices. Different to the existing literature that focus on comparing different models' option pricing performance by using the same SPX and VIX information, e.g., Kaeck and Alexander (2012) and Yang and Kanninen (2017), this paper

newly investigates whether adding the new indices can further improve models' option pricing performance. After we have well known how to choose a good model, choosing the informative data for option prices becomes more and more important. Recently, Bardgett et al. (2018) document that adding VIX option data to calibrate the affine models can significantly improve the return predictability of the model-implied variance risk premium. We need to carefully choose the data used to calibrate the models for different models and purposes.

Even though, the answer of whether adding the new indices can further improve models' option pricing performance depends on the model we choose, roughly speaking, our studies send two important messages: the CBOE VIX is a very informative index but the CBOE SKEW is a very noisy index for option prices; the VIX term structure is informative for some models. Considering the information embedded in the CBOE VIX Volatility Index (VVIX) for the SPX option prices can be further investigated. Nevertheless, our current paper pays attention on the importance of choosing indices for the model calibration in terms of inferring information for the option prices.

Appendix A: Proofs

A.1 CBOE VIX

In order to calculate the VIX under the SVCJH model, we need the following lemma studied by Dassios and Zhao (2011).

Lemma 1. *For $s > t > 0$, given the Hawkes process in Table 2, the conditional expectation of $\lambda_s^{\mathbb{Q}}$ on \mathcal{F}_t under the risk-neutral measure \mathbb{Q} is*

$$E_t^{\mathbb{Q}}(\lambda_s^{\mathbb{Q}}) = \lambda_t^{\mathbb{Q}} e^{-\alpha^{\mathbb{Q}}(s-t)} + \bar{\lambda}^{\mathbb{Q}} \left(1 - e^{-\alpha^{\mathbb{Q}}(s-t)}\right), \quad (16)$$

where $\bar{\lambda}^{\mathbb{Q}} = \lambda_{\infty}^{\mathbb{Q}} \beta / \alpha^{\mathbb{Q}}$ and $\alpha^{\mathbb{Q}} = \beta - \mu_z^{\mathbb{Q}} > 0$. If $\beta = \mu_z^{\mathbb{Q}}$, then

$$E_t^{\mathbb{Q}}(\lambda_s^{\mathbb{Q}}) = \lambda_t^{\mathbb{Q}} + \lambda_{\infty}^{\mathbb{Q}} \beta (s-t). \quad (17)$$

Obviously, for $\alpha^{\mathbb{Q}} = \beta - \mu_z^{\mathbb{Q}} > 0$, the unconditional expectation of $\lambda_t^{\mathbb{Q}}$ is

$$E(\lambda_t^{\mathbb{Q}}) = \bar{\lambda}^{\mathbb{Q}} = \frac{\lambda_{\infty}^{\mathbb{Q}} \beta}{\alpha^{\mathbb{Q}}}. \quad (18)$$

Given the volatility process in Equation (3), for $s > t > 0$, applying Itô's lemma to $e^{\kappa^{\mathbb{Q}} t} v_t$ leads to

$$v_s = e^{-\kappa^{\mathbb{Q}}(s-t)} v_t + \frac{\kappa \theta}{\kappa^{\mathbb{Q}}} \left(1 - e^{-\kappa^{\mathbb{Q}}(s-t)}\right) + \int_t^s e^{-\kappa^{\mathbb{Q}}(s-u)} \sigma_v \sqrt{v_u} dW_{u,v}^{\mathbb{Q}} + \int_t^s e^{-\kappa^{\mathbb{Q}}(s-u)} y dN_u. \quad (19)$$

Using Lemma 1, we have

$$\begin{aligned} E_t^{\mathbb{Q}}(v_s) &= e^{-\kappa^{\mathbb{Q}}(s-t)} v_t + \frac{\kappa \theta}{\kappa^{\mathbb{Q}}} \left(1 - e^{-\kappa^{\mathbb{Q}}(s-t)}\right) \\ &\quad + \mu_y^{\mathbb{Q}} \int_t^s e^{-\kappa^{\mathbb{Q}}(s-u)} \left[\lambda_t^{\mathbb{Q}} e^{-\alpha^{\mathbb{Q}}(u-t)} + \bar{\lambda}^{\mathbb{Q}} \left(1 - e^{-\alpha^{\mathbb{Q}}(u-t)}\right) \right] du \\ &= e^{-\kappa^{\mathbb{Q}}(s-t)} v_t + \frac{\kappa \theta}{\kappa^{\mathbb{Q}}} \left(1 - e^{-\kappa^{\mathbb{Q}}(s-t)}\right) + \frac{\mu_y^{\mathbb{Q}}}{\kappa^{\mathbb{Q}} - \alpha^{\mathbb{Q}}} \left(e^{-\alpha^{\mathbb{Q}}(s-t)} - e^{-\kappa^{\mathbb{Q}}(s-t)}\right) \lambda_t^{\mathbb{Q}} \\ &\quad + \frac{\mu_y^{\mathbb{Q}} \bar{\lambda}^{\mathbb{Q}}}{\kappa^{\mathbb{Q}}} \left(1 - e^{-\kappa^{\mathbb{Q}}(s-t)}\right) - \frac{\mu_y^{\mathbb{Q}} \bar{\lambda}^{\mathbb{Q}}}{\kappa^{\mathbb{Q}} - \alpha^{\mathbb{Q}}} \left(e^{-\alpha^{\mathbb{Q}}(s-t)} - e^{-\kappa^{\mathbb{Q}}(s-t)}\right). \end{aligned}$$

Then, for $\kappa^{\mathbb{Q}} \neq \alpha^{\mathbb{Q}}$,

$$\begin{aligned}
\bar{v}_{t,t+\tau}^{\mathbb{Q}} &= \frac{1}{\tau} E_t^{\mathbb{Q}} \left(\int_t^{t+\tau} v_s ds \right) = \frac{1}{\tau} \int_t^{t+\tau} E_t^{\mathbb{Q}}(v_s) ds \\
&= \frac{1 - e^{-\kappa^{\mathbb{Q}}\tau}}{\kappa^{\mathbb{Q}}\tau} v_t + \frac{\kappa\theta + \mu_y^{\mathbb{Q}}\bar{\lambda}^{\mathbb{Q}}}{\kappa^{\mathbb{Q}}} \left(1 - \frac{1 - e^{-\kappa^{\mathbb{Q}}\tau}}{\kappa^{\mathbb{Q}}\tau} \right) \\
&\quad + \frac{\mu_y^{\mathbb{Q}}(\lambda_t^{\mathbb{Q}} - \bar{\lambda}^{\mathbb{Q}})}{\kappa^{\mathbb{Q}} - \alpha^{\mathbb{Q}}} \left(\frac{1 - e^{-\alpha^{\mathbb{Q}}\tau}}{\alpha^{\mathbb{Q}}\tau} - \frac{1 - e^{-\kappa^{\mathbb{Q}}\tau}}{\kappa^{\mathbb{Q}}\tau} \right) \\
&= \varphi_{\kappa^{\mathbb{Q}},\tau} v_t + \frac{\kappa\theta + \mu_y^{\mathbb{Q}}\bar{\lambda}^{\mathbb{Q}}}{\kappa^{\mathbb{Q}}} (1 - \varphi_{\kappa^{\mathbb{Q}},\tau}) + \frac{\mu_y^{\mathbb{Q}}(\lambda_t^{\mathbb{Q}} - \bar{\lambda}^{\mathbb{Q}})}{\kappa^{\mathbb{Q}} - \alpha^{\mathbb{Q}}} (\varphi_{\alpha^{\mathbb{Q}},\tau} - \varphi_{\kappa^{\mathbb{Q}},\tau}),
\end{aligned}$$

where $\varphi_{a,\tau} = \frac{1 - e^{-a\tau}}{a\tau}$.

Furthermore,

$$\begin{aligned}
\frac{1}{\tau} E_t^{\mathbb{Q}} \left(\int_t^{t+\tau} \lambda_s^{\mathbb{Q}} ds \right) &= \frac{1}{\tau} \int_t^{t+\tau} E_t^{\mathbb{Q}}(\lambda_s^{\mathbb{Q}}) ds = \frac{1 - e^{-\alpha^{\mathbb{Q}}\tau}}{\alpha^{\mathbb{Q}}\tau} \lambda_t^{\mathbb{Q}} + \bar{\lambda}^{\mathbb{Q}} \left(1 - \frac{1 - e^{-\alpha^{\mathbb{Q}}\tau}}{\alpha^{\mathbb{Q}}\tau} \right) \\
&= \varphi_{\alpha^{\mathbb{Q}},\tau} \lambda_t^{\mathbb{Q}} + \bar{\lambda}^{\mathbb{Q}} (1 - \varphi_{\alpha^{\mathbb{Q}},\tau}).
\end{aligned}$$

Finally, under the risk neutral measure, a CBOE VIX formula can be obtained by

$$\begin{aligned}
VIX_{t,\tau}^2 &= \frac{1}{\tau} E_t^{\mathbb{Q}} \left(\int_t^{t+\tau} v_s ds \right) + \frac{2}{\tau} \left(e^{\mu_x^{\mathbb{Q}} + \sigma_x^2/2} - 1 - \mu_x^{\mathbb{Q}} \right) E_t^{\mathbb{Q}} \left(\int_t^{t+\tau} \lambda_s^{\mathbb{Q}} ds \right) \\
&= \bar{v}_{t,t+\tau}^{\mathbb{Q}} + 2 \left(e^{\mu_x^{\mathbb{Q}} + \sigma_x^2/2} - 1 - \mu_x^{\mathbb{Q}} \right) \left[\varphi_{\alpha^{\mathbb{Q}},\tau} \lambda_t^{\mathbb{Q}} + \bar{\lambda}^{\mathbb{Q}} (1 - \varphi_{\alpha^{\mathbb{Q}},\tau}) \right].
\end{aligned}$$

For the SVCJ and SVCJI models, using $\lambda_t^{\mathbb{Q}} = \eta^\lambda \lambda_t = \lambda_1^{\mathbb{Q}} + \lambda_2^{\mathbb{Q}} v_t$, we denote $\tilde{\kappa}^{\mathbb{Q}} = \kappa^{\mathbb{Q}} - \mu_y^{\mathbb{Q}} \lambda_2^{\mathbb{Q}}$

and then

$$E_t^{\mathbb{Q}}(v_s) = e^{-\tilde{\kappa}^{\mathbb{Q}}(s-t)} v_t + \frac{\kappa\theta + \mu_y^{\mathbb{Q}}\lambda_1^{\mathbb{Q}}}{\tilde{\kappa}^{\mathbb{Q}}} \left(1 - e^{-\tilde{\kappa}^{\mathbb{Q}}(s-t)} \right). \quad (20)$$

We obtain

$$\bar{v}_{t,t+\tau}^{\mathbb{Q}} = \frac{1}{\tau} E_t^{\mathbb{Q}} \left(\int_t^{t+\tau} v_s ds \right) = \varphi_{\tilde{\kappa}^{\mathbb{Q}},\tau} v_t + \frac{\kappa\theta + \mu_y^{\mathbb{Q}}\lambda_1^{\mathbb{Q}}}{\tilde{\kappa}^{\mathbb{Q}}} (1 - \varphi_{\tilde{\kappa}^{\mathbb{Q}},\tau}). \quad (21)$$

Finally, we get

$$\begin{aligned} VIX_{t,\tau}^2 &= \frac{1}{\tau} E_t^{\mathbb{Q}} \left(\int_t^{t+\tau} v_s ds \right) + \frac{2}{\tau} \left(e^{\mu_x^{\mathbb{Q}} + \sigma_x^2/2} - 1 - \mu_x^{\mathbb{Q}} \right) E_t^{\mathbb{Q}} \left(\int_t^{t+\tau} \lambda_s^{\mathbb{Q}} ds \right) \\ &= \bar{v}_{t,t+\tau}^{\mathbb{Q}} + 2 \left(e^{\mu_x^{\mathbb{Q}} + \sigma_x^2/2} - 1 - \mu_x^{\mathbb{Q}} \right) \left(\lambda_1^{\mathbb{Q}} + \lambda_2^{\mathbb{Q}} \bar{v}_{t,t+\tau}^{\mathbb{Q}} \right) \end{aligned}$$

A.2 MGF

Under the SVCJH model, denoting $X_t = \log S_t$, then

$$\begin{cases} dX_t = \left(r - q - \frac{1}{2}v_t - \lambda_t^{\mathbb{Q}} m^{\mathbb{Q}} \right) dt + \sqrt{v_t} dW_{t,S}^{\mathbb{Q}} + x dN_t, \\ dv_t = \kappa^{\mathbb{Q}} (\kappa\theta/\kappa^{\mathbb{Q}} - v_t) dt + \sigma_v \sqrt{v_t} dW_{t,v}^{\mathbb{Q}} + y dN_t, \\ d\lambda_t^{\mathbb{Q}} = \beta(\lambda_{\infty}^{\mathbb{Q}} - \lambda_t^{\mathbb{Q}}) dt + z dN_t. \end{cases} \quad (22)$$

The moment generating function (MGF) of X_T can be defined as $f(\omega, t, ; X, v, \lambda^{\mathbb{Q}}) = E_t^{\mathbb{Q}}[e^{\omega X_T}]$.

It is a martingale and satisfies the following partial differential equation (PDE),

$$\begin{cases} 0 = \frac{\partial f}{\partial t} + \frac{\partial f}{\partial X} \left(r - q - \frac{1}{2}v - \lambda^{\mathbb{Q}} m^{\mathbb{Q}} \right) + \frac{1}{2} \frac{\partial^2 f}{\partial X^2} v + \frac{\partial^2 f}{\partial X v} \rho \sigma_v v + \frac{\partial f}{\partial v} \kappa^{\mathbb{Q}} (\kappa\theta/\kappa^{\mathbb{Q}} - v) \\ \quad + \frac{1}{2} \frac{\partial^2 f}{\partial v^2} \sigma_v^2 v + \frac{\partial f}{\partial \lambda^{\mathbb{Q}}} \beta(\lambda_{\infty}^{\mathbb{Q}} - \lambda^{\mathbb{Q}}) + \lambda^{\mathbb{Q}} E^{\mathbb{Q}} [f(X + x, v + y, \lambda^{\mathbb{Q}} + z) - f] \\ f(T, X, v, \lambda^{\mathbb{Q}}) = e^{\omega X}. \end{cases} \quad (23)$$

If we denote $\tau = T - t$, then the above PDE can be rewritten as

$$\begin{cases} \frac{\partial f}{\partial \tau} = \frac{\partial f}{\partial X} \left(r - q - \frac{1}{2}v - \lambda^{\mathbb{Q}} m^{\mathbb{Q}} \right) + \frac{1}{2} \frac{\partial^2 f}{\partial X^2} v + \frac{\partial^2 f}{\partial X v} \rho \sigma_v v + \frac{\partial f}{\partial v} \kappa^{\mathbb{Q}} (\kappa\theta/\kappa^{\mathbb{Q}} - v) \\ \quad + \frac{1}{2} \frac{\partial^2 f}{\partial v^2} \sigma_v^2 v + \frac{\partial f}{\partial \lambda^{\mathbb{Q}}} \beta(\lambda_{\infty}^{\mathbb{Q}} - \lambda^{\mathbb{Q}}) + \lambda^{\mathbb{Q}} E^{\mathbb{Q}} [f(X + x, v + y, \lambda^{\mathbb{Q}} + z) - f] \\ f(0, X, v, \lambda^{\mathbb{Q}}) = e^{\omega X}. \end{cases} \quad (24)$$

Now we guess the solution of the above PDE has the following form,

$$f(\omega, \tau) = e^{A(\omega, \tau) + B(\omega, \tau)v_t + C(\omega, \tau)\lambda_t^{\mathbb{Q}} + \omega X_t}. \quad (25)$$

Then $A(\omega, \tau)$, $B(\omega, \tau)$ and $C(\omega, \tau)$ satisfy the following ordinary differential equations (ODEs)

$$\frac{\partial A(\omega, \tau)}{\partial \tau} = B(\omega, \tau)\kappa\theta + \omega(r - q) + C(\omega, \tau)\beta\lambda_{\infty}^{\mathbb{Q}}, \quad (26)$$

$$\frac{\partial B(\omega, \tau)}{\partial \tau} = \frac{1}{2}B^2(\omega, \tau)\sigma_v^2 - (\kappa^{\mathbb{Q}} - \rho\sigma_v\omega)B(\omega, \tau) - \frac{1}{2}(\omega - \omega^2), \quad (27)$$

$$\frac{\partial C(\omega, \tau)}{\partial \tau} = -\omega m^{\mathbb{Q}} - C(\omega, \tau)\beta + \frac{e^{\omega\mu_x^{\mathbb{Q}} + \frac{1}{2}\omega^2\sigma_x^2}}{(1 - B(\omega, \tau)\mu_y^{\mathbb{Q}})(1 - C(\omega, \tau)\mu_z^{\mathbb{Q}})} - 1, \quad (28)$$

with the initial conditions $A(\omega, 0) = 0, B(\omega, 0) = 0, C(\omega, 0) = 0$.

Under the SVCJI model, $f(\omega, \tau) = e^{A(\omega, \tau) + B(\omega, \tau)v_t + \omega X_t}$ where Then $A(\omega, \tau), B(\omega, \tau)$ satisfy the following ordinary differential equations (ODEs)

$$\frac{\partial A(\omega, \tau)}{\partial \tau} = B(\omega, \tau)\kappa\theta + \omega(r - q) - \omega m^{\mathbb{Q}}\lambda_1^{\mathbb{Q}} + \lambda_1^{\mathbb{Q}} \left(\frac{e^{\omega\mu_x^{\mathbb{Q}} + \frac{1}{2}\omega^2\sigma_x^2}}{1 - B(\omega, \tau)\mu_y^{\mathbb{Q}}} - 1 \right), \quad (29)$$

$$\begin{aligned} \frac{\partial B(\omega, \tau)}{\partial \tau} = & \frac{1}{2}B^2(\omega, \tau)\sigma_v^2 - (\kappa^{\mathbb{Q}} - \rho\sigma_v\omega)B(\omega, \tau) - \frac{1}{2}(\omega - \omega^2) \\ & - \omega m^{\mathbb{Q}}\lambda_2^{\mathbb{Q}} + \lambda_2^{\mathbb{Q}} \left(\frac{e^{\omega\mu_x^{\mathbb{Q}} + \frac{1}{2}\omega^2\sigma_x^2}}{1 - B(\omega, \tau)\mu_y^{\mathbb{Q}}} - 1 \right), \end{aligned} \quad (30)$$

with the initial conditions $A(\omega, 0) = 0, B(\omega, 0) = 0$.

Under the SVCJ model, $A(\omega, \tau)$ and $B(\omega, \tau)$ have closed-form solutions, i.e.,

$$B(\omega, \tau) = \frac{-(\omega - \omega^2)(1 - e^{-\zeta\tau})}{\xi_+ e^{-\zeta\tau} + \xi_-},$$

where

$$\zeta = \sqrt{(\kappa^{\mathbb{Q}} - \rho\sigma_v\omega)^2 + \sigma_v^2(\omega - \omega^2)}, \quad \xi_{\pm} = \zeta \mp (\kappa^{\mathbb{Q}} - \rho\sigma_v\omega),$$

and

$$\begin{aligned}
A(\omega, \tau) &= \kappa\theta \int_0^\tau B(\omega, u) du + (r - q)\omega\tau - \lambda_1^{\mathbb{Q}} \omega m^{\mathbb{Q}} \tau + \lambda_1^{\mathbb{Q}} \int_0^\tau \left(\frac{e^{\omega\mu_x^{\mathbb{Q}} + \frac{1}{2}\omega^2\sigma_x^2}}{1 - B(\omega, u)\mu_y^{\mathbb{Q}}} - 1 \right) du \\
&= -\frac{\kappa\theta}{\sigma_v^2} \left(\xi_+ \tau + 2 \ln \frac{\xi_+ e^{-\zeta\tau} + \xi_-}{2\zeta} \right) + (r - q)\omega\tau \\
&\quad - \lambda_1^{\mathbb{Q}} \left(\omega m^{\mathbb{Q}} + 1 \right) \tau + \lambda_1^{\mathbb{Q}} e^{\omega\mu_x^{\mathbb{Q}} + \frac{1}{2}\omega^2\sigma_x^2} \int_0^\tau \frac{1}{1 - B(\omega, u)\mu_y^{\mathbb{Q}}} du,
\end{aligned}$$

where

$$\begin{aligned}
\int_0^\tau \frac{1}{1 - B(\omega, u)\mu_y^{\mathbb{Q}}} du &= \int_0^\tau \frac{\xi_+ e^{-\zeta u} + \xi_-}{\left(\xi_+ - \mu_y^{\mathbb{Q}}(\omega - \omega^2) \right) e^{-\zeta u} + \left(\xi_- + \mu_y^{\mathbb{Q}}(\omega - \omega^2) \right)} du \\
&= \frac{\xi_-}{\xi_- + \mu_y^{\mathbb{Q}}(\omega - \omega^2)} \tau - \frac{1}{\zeta} \left(\frac{\xi_+}{\xi_+ - \mu_y^{\mathbb{Q}}(\omega - \omega^2)} - \frac{\xi_-}{\xi_- + \mu_y^{\mathbb{Q}}(\omega - \omega^2)} \right) \\
&\quad \cdot \ln \frac{\left(\xi_+ - \mu_y^{\mathbb{Q}}(\omega - \omega^2) \right) e^{-\zeta\tau} + \left(\xi_- + \mu_y^{\mathbb{Q}}(\omega - \omega^2) \right)}{2\zeta}.
\end{aligned}$$

A.3 Option prices

We define the European call option price at time 0 as

$$C_0 = E_0^{\mathbb{Q}} \left[e^{-rT} (S_T - K)^+ \right] = E_0^{\mathbb{Q}} \left[e^{-rT} \left(e^{\log S_T} - e^k \right)^+ \right], \quad (31)$$

where $k = \log K$ and K is the strike price, T is the maturity date, $(\cdot)^+$ denotes $\max\{\cdot, 0\}$ and $(S_T - K)^+$ is the payoff function of the call option at the maturity date.

Following Carr and Madan (1999), we rewrite the option price as $\hat{C}_0(k) = e^{\alpha k} C_0$ for $\alpha > 0$, so that $C_0 = e^{-\alpha k} \hat{C}_0(k)$, which can be derived as

$$C_0(k) = e^{-\alpha k} \left[\frac{1}{2\pi} \int_{-\infty}^{+\infty} e^{-iuk} \left(\int_{-\infty}^{+\infty} e^{iuk} \hat{C}_0(k) dk \right) du \right] = \frac{e^{-\alpha k}}{\pi} \int_0^{+\infty} e^{-iuk} \phi(u) du, \quad (32)$$

where $\phi(u) = \frac{e^{-rT} f_T(iu + (1+\alpha))}{\alpha^2 + \alpha - u^2 + i(2\alpha + 1)u}$ and $f_T(\omega) = f(T, X, v, \lambda^{\mathbb{Q}}) = E_0^{\mathbb{Q}}[e^{\omega X_T}]$.

Following Carr and Madan (1999), we adopt the trapezoid rule for the integral by setting $u_j = \Delta_u(j - 1)$ where $j = 1, \dots, N$ and Δ_u is the grid spacing. The value of Δ_u should be sufficiently small to approximate the integral well enough, while the value of $N\Delta_u$ should be

large enough to assume that the characteristic function is equal to zero for $u > N\Delta_u$. The approximation of the option price in Equation (32) can be obtained as

$$\begin{aligned} C_0(k) &\approx \frac{e^{-\alpha k}}{\pi} \left(\frac{1}{2} e^{-iu_1 k} \phi(u_1) + \sum_{j=2}^{N-1} e^{-iu_j k} \phi(u_j) + \frac{1}{2} e^{-iu_N k} \phi(u_N) \right) \Delta_u \\ &= \frac{e^{-\alpha k}}{\pi} \sum_{j=1}^N q_j e^{-iu_j k} \phi(u_j) \Delta_u, \end{aligned} \quad (33)$$

where $q_1 = q_N = \frac{1}{2}$ and $q_j = 1$ for $2 \leq j \leq N - 1$.

Put option prices can be calculated from the put-call parity.

Appendix B: Technical notes on MCMC with the CBOE SKEW

For the MCMC, we rely on the `rjags` package, which provides an interface from R to the JAGS library for Bayesian data analysis. JAGS is a clone of BUGS (Bayesian analysis Using Gibbs Sampling). For details, see <https://cran.r-project.org/web/packages/rjags/index.html>. The DIC value computed follows a standard way, e.g., Appendix C in Yang and Kannianen (2017).

We use the Runge–Kutta (RK4) numerical method to solve ODEs (26)–(28) in R. Let an initial value problem be specified as follows:

$$y' = f(t, y), \quad y(t_0) = y_0.$$

Here y is an unknown function (scalar or vector) of time t , which we would like to approximate; we are told that y' , the rate at which y changes, is a function of t and of y itself. At the initial time t_0 the corresponding y value is y_0 . The function f and the data t_0, y_0 are given.

Now pick a step-size $h > 0$ and define

$$\begin{aligned} y_{n+1} &= y_n + \frac{1}{6} (k_1 + 2k_2 + 2k_3 + k_4), \\ t_{n+1} &= t_n + h \end{aligned}$$

for $n = 0, 1, 2, 3, \dots$, using

$$\begin{aligned} k_1 &= h f(t_n, y_n), \\ k_2 &= h f\left(t_n + \frac{h}{2}, y_n + \frac{k_1}{2}\right), \\ k_3 &= h f\left(t_n + \frac{h}{2}, y_n + \frac{k_2}{2}\right), \\ k_4 &= h f(t_n + h, y_n + k_3). \end{aligned}$$

We use the central finite differences to approximate A_2, B_2, C_2, A_3, B_3 and C_3 with the spacing of 0.01 for ω in \mathbb{R} . For example, A_2 and A_3 can be approximated by

$$\begin{aligned} A_2 &= \left. \frac{\partial^2 A(\tau, \omega)}{\partial \omega^2} \right|_{\omega=0} \approx \frac{A(-d, \tau) + A(d, \tau)}{d^2}, \\ A_3 &= \left. \frac{\partial^3 A(\tau, \omega)}{\partial \omega^3} \right|_{\omega=0} \approx \frac{-\frac{1}{2}A(-2d, \tau) + A(-d, \tau) - A(d, \tau) + \frac{1}{2}A(2d, \tau)}{d^3}, \end{aligned}$$

where $d = 0.01$.

Appendix C: Fit of CBOE indices

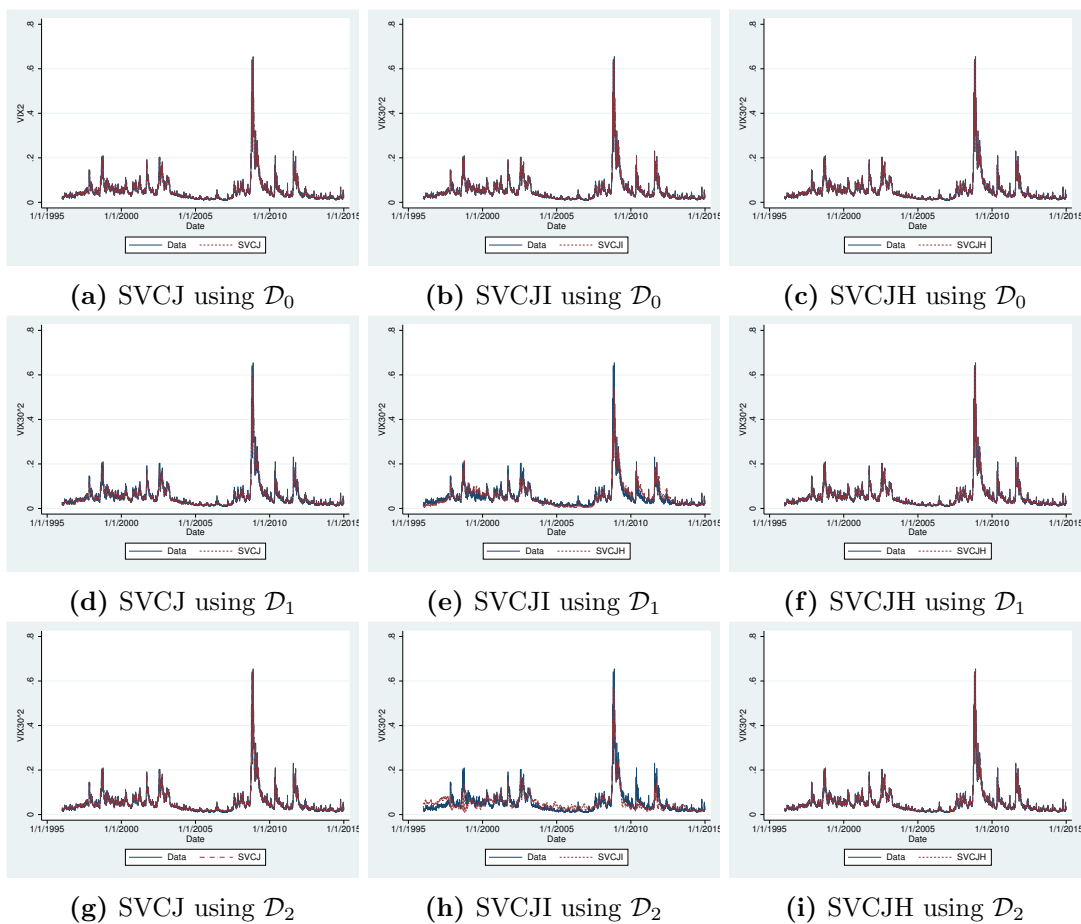


Figure 3: Fit of $VIX_{t,30}^2$. Data are from 02 January 1996 to 31 December 2014.

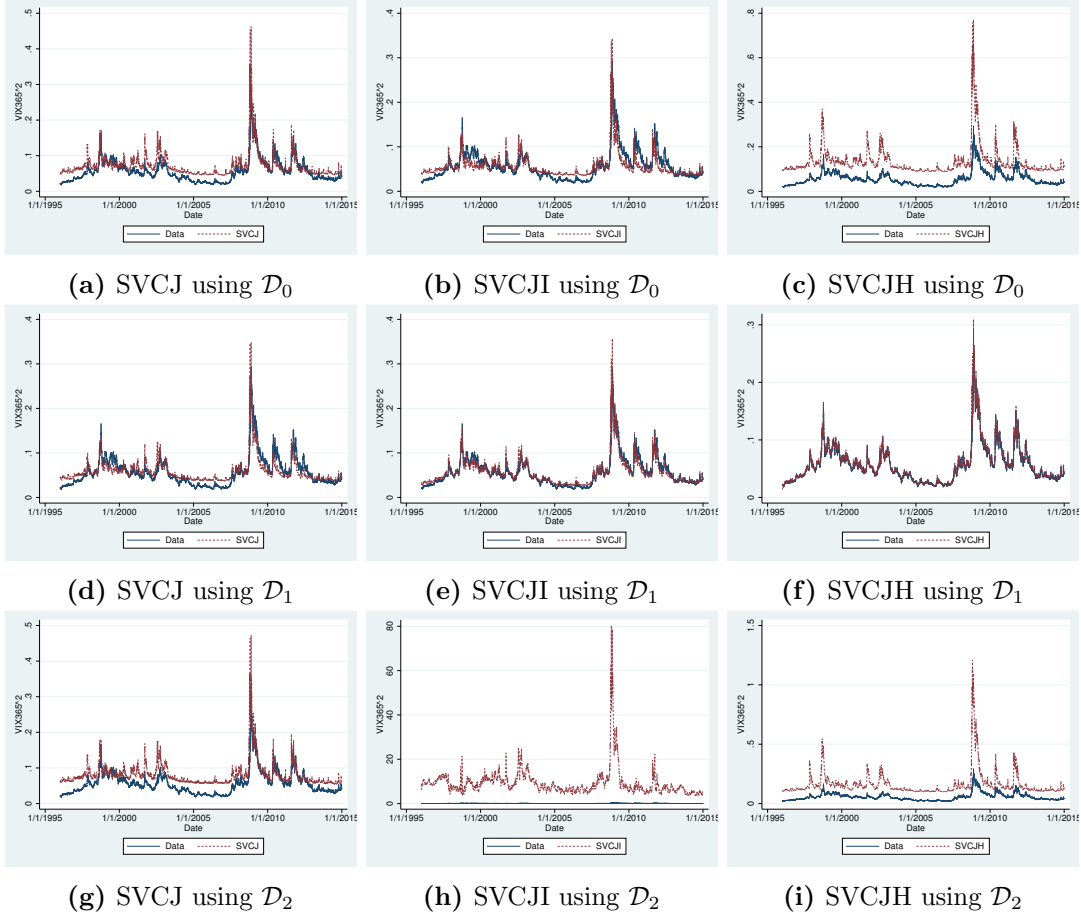


Figure 4: Fit of $VIX_{t,365}^2$. Data are from 02 January 1996 to 31 December 2014.

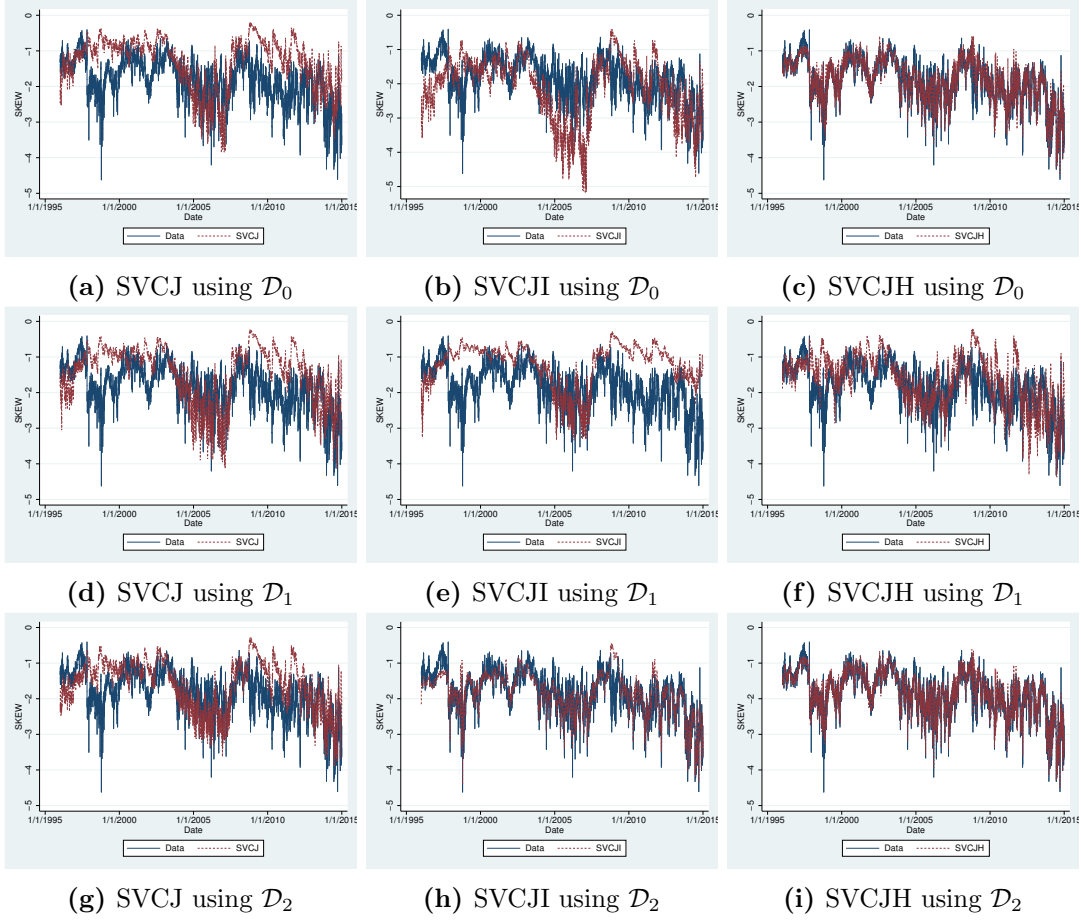


Figure 5: Fit of $SKEW_{t,30}$. Data are from 02 January 1996 to 31 December 2014.

References

- Aït-Sahalia, Yacine, Mustafa Karaman, and Lorian Mancini, 2015, The term structure of variance swaps and risk premia, Available at SSRN 2136820.
- Bakshi, Gurdip, Charles Cao, and Zhiwu Chen, 1997, Empirical performance of alternative option pricing models, *Journal of Finance* 52, 2003–2049.
- Bakshi, Gurdip, Nikunj Kapadia, and Dilip Madan, 2003, Stock return characteristics, skew laws, and the differential pricing of individual equity options, *Review of Financial Studies* 16, 101–143.
- Bardgett, Chris, Elise Gourier, and Markus Leippold, 2018, Inferring volatility dynamics and risk premia from the S&P 500 and VIX markets, *Journal of Financial Economics*, forthcoming.
- Bates, David S, 2006, Maximum likelihood estimation of latent affine processes, *Review of Financial Studies* 19, 909–965.
- Black, Fischer, and Myron Scholes, 1973, The pricing of options and corporate liabilities, *Journal of Political Economy* 637–654.
- Bollerslev, Tim, and Viktor Todorov, 2011, Tails, fears, and risk premia, *Journal of Finance* 66, 2165–2211.
- Broadie, Mark, Mikhail Chernov, and Michael Johannes, 2007, Model specification and risk premia: Evidence from futures options, *Journal of Finance* 62, 1453–1490.
- Carr, Peter, and Dilip Madan, 1999, Option valuation using the fast fourier transform, *Journal of Computational Finance* 2, 61–73.
- Carr, Peter, and Liuren Wu, 2016, Analyzing volatility risk and risk premium in option contracts: A new theory, *Journal of Financial Economics* 120, 1–20.
- Da Fonseca, José, and Katja Ignatieva, 2019, Jump activity analysis for affine jump-diffusion models: Evidence from the commodity market, *Journal of Banking and Finance* 99, 45–62.

- Dassios, Angelos, and Hongbiao Zhao, 2011, A dynamic contagion process, *Advances in Applied Probability* 43, 814–846.
- Drechsler, Itamar, 2013, Uncertainty, time-varying fear, and asset prices, *Journal of Finance* 68, 1843–1889.
- Drechsler, Itamar, and Amir Yaron, 2010, What’s vol got to do with it, *Review of Financial Studies* 24, 1–45.
- Du, Du, and Dan Luo, 2017, The pricing of jump propagation: Evidence from spot and options markets, *Management Science*, forthcoming.
- Duan, Jin-Chuan, and Chung-Ying Yeh, 2010, Jump and volatility risk premiums implied by VIX, *Journal of Economic Dynamics and Control* 34, 2232–2244.
- Duffie, Darrell, Jun Pan, and Kenneth Singleton, 2000, Transform analysis and asset pricing for affine jump-diffusions, *Econometrica* 68, 1343–1376.
- Egloff, Daniel, Markus Leippold, and Liuren Wu, 2010, The term structure of variance swap rates and optimal variance swap investments, *Journal of Financial and Quantitative Analysis* 1279–1310.
- Eraker, Bjørn, 2004, Do stock prices and volatility jump? reconciling evidence from spot and option prices, *Journal of Finance* 59, 1367–1404.
- Eraker, Bjørn, Michael Johannes, and Nicholas Polson, 2003, The impact of jumps in volatility and returns, *Journal of Finance* 58, 1269–1300.
- Eraker, Bjørn, and Ivan Shaliastovich, 2008, An equilibrium guide to designing affine pricing models, *Mathematical Finance* 18, 519–543.
- Heston, Steven L, 1993, A closed-form solution for options with stochastic volatility with applications to bond and currency options, *Review of Financial Studies* 6, 327–343.
- Jacquier, Eric, Nicholas G Polson, and Peter E Rossi, 2002, Bayesian analysis of stochastic volatility models, *Journal of Business and Economic Statistics* 20, 69–87.

- Jiang, George J, and Yisong S Tian, 2005, The model-free implied volatility and its information content, *Review of Financial Studies* 18, 1305–1342.
- Jin, Jianjian, 2014, Jump-diffusion long-run risks models, variance risk premium, and volatility dynamics, *Review of Finance* 19, 1223–1279.
- Johannes, Michael, and Nicholas Polson, 2009, MCMC methods for continuous-time financial econometrics, *Handbook of Financial Econometrics* .
- Kaeck, Andreas, and Carol Alexander, 2012, Volatility dynamics for the S&P 500: Further evidence from non-affine, multi-factor jump diffusions, *Journal of Banking and Finance* 36, 3110–3121.
- Kaeck, Andreas, Paulo Rodrigues, and Norman J Seeger, 2017, Equity index variance: Evidence from flexible parametric jump–diffusion models, *Journal of Banking and Finance* 83, 85–103.
- Li, Junye, and Gabriele Zinna, 2018, The variance risk premium: Components, term structures, and stock return predictability, *Journal of Business and Economic Statistics* 36, 411–425.
- Lin, Yueh-Neng, 2007, Pricing VIX futures: Evidence from integrated physical and risk-neutral probability measures, *Journal of Futures Markets* 27, 1175–1217.
- Lin, Yueh-Neng, and Chien-Hung Chang, 2010, Consistent modeling of s&p 500 and vix derivatives, *Journal of Economic Dynamics and Control* 34, 2302–2319.
- Liu, Zhangxin Frank, and Thijs van der Heijden, 2016, Model-free risk-neutral moments and proxies, Available at SSRN 2641559.
- Neuberger, Anthony, 2012, Realized skewness, *Review of Financial Studies* 25, 3423–3455.
- Neumann, Maximilian, Marcel Prokopczuk, and Chardin Wese Simen, 2016, Jump and variance risk premia in the S&P 500, *Journal of Banking and Finance* 69, 72–83.
- Ruan, Xinfeng, and Jin E Zhang, 2018, Equilibrium variance risk premium in a cost-free production economy, *Journal of Economic Dynamics and Control* 96, 42–60.

- Todorov, Viktor, 2010, Variance risk-premium dynamics: The role of jumps, *Review of Financial Studies* 23, 345–383.
- Yang, Hanxue, and Juho Kanniainen, 2017, Jump and volatility dynamics for the S&P 500: Evidence for infinite-activity jumps with non-affine volatility dynamics from stock and option markets, *Review of Finance* 21, 811–844.
- Zhang, Jin E, Fang Zhen, Xiaoxia Sun, and Huimin Zhao, 2017, The skewness implied in the Heston model and its application, *Journal of Futures Markets* 37, 211–237.
- Zhu, Song-Ping, and Guang-Hua Lian, 2011, A closed-form exact solution for pricing variance swaps with stochastic volatility, *Mathematical Finance* 21, 233–256.
- Zhu, Song-Ping, and Guang-Hua Lian, 2012, An analytical formula for VIX futures and its applications, *Journal of Futures Markets* 32, 166–190.